



Review

Recent advances in application of polypyrrole nanomaterial in water pollution control

Weilai Wang^{*}, Yaping Lv, Haijin Liu, Zhiguo Cao^{*}

Ministry of Education Key Laboratory for Yellow River and Huai River Water Environment and Pollution Control, School of Environment, Henan Normal University, Xinxiang, Henan 453007, China

ARTICLE INFO

Editor: Z Bao

Keywords:

Polypyrrole
Water pollution control
Separation and purification
Oxidation and reduction
Antibacterial and disinfection

ABSTRACT

Faced with the complex and severe water pollution situation, various water treatment technologies are developing rapidly. Environmental functional materials, as the material foundation for technological development, have received increasing attention. Polypyrrole is a black conductive polymer, which can be easily obtained through the oxidation polymerization of pyrrole monomer. Polypyrrole has the characteristics of nontoxicity, low density, high purity, light absorption, electric conductivity, antibacterial, corrosion resistance, modifiability, and is therefore widely used in water treatment technologies. This work summarizes the research achievements of polypyrrole in water pollution control technologies such as separation and purification, oxidation and reduction, antibacterial and disinfection in the past decade. Specifically, the synthesis methods, modification strategies, and application scenarios of polypyrrole are introduced; the direct and indirect action mechanisms in corresponding water treatment technologies of polypyrrole are analysis, and the relationship between structural properties and application technology of polypyrrole is established. Moreover, a critical summary of the current research advances of polypyrrole was conducted, and potential future research and development direction are prospected.

1. Introduction

Water is not only essential for sustaining life, but it is also a common hiding place for dirt and pollutants. As we all know, water pollution can be attributed to both natural and human factors. However, with the rapid development of industrialization, human activities have significantly contributed to the deterioration of water quality, resulting in increasingly complex and severe water pollution [1]. The types of pollutants that contaminate water can be classified into inorganic compounds (such as heavy metals, acid-base salts, and radionuclides), organic pollutants (such as pesticides, pharmaceuticals, and chemical raw materials), and microbial pollutants (bacteria and viruses) [2].

Various water pollution control technologies have been researched and developed based on the unique characteristics of different pollution sources. These technologies include separation and purification, oxidation and reduction, antibacterial and disinfection. Materials, as vital carriers for these technologies, have been extensively studied, such as carbon materials (graphene, carbon nanotubes, and biochar) [3], semiconductor materials (metal oxides, metal sulfides, and metal phosphides) [4], as well as organic polymer materials (chitosan,

cellulose, and dopamine) [5]. Notably, conductive polymers exhibit the characteristics (mechanical stability, photoelectric characteristics, flexible) of the above three types of materials [6], and are receiving increasing research attention.

Common conductive polymers include polyacetylene, polypyrrole, polythiophene, polyaniline, polyphenylene, etc. Among them, polypyrrole (black), polythiophene (red) and polyaniline (mottled) with heteroatoms increase the electron cloud density of the polymer and activate it, showing excellent physical and chemical properties [7]. Especially, polypyrrole (PPy) is inexpensive, non-toxic, easy to obtain, and has excellent light absorption, electric conductivity and biocompatibility, making it an ideal environmental functional material (Fig. 1).

In recent years, the annual publication volume of PPy has remained stable at around 1500, with approximately 300 publications related to water (Fig. 2). Although several review articles on PPy water pollution control have been published, they mainly focus on a certain type of PPy-based material, the treatment of a specific pollutant, or the research application in a particular technology [8–11]. However, there is a lack of a comprehensive review report on PPy in the field of water pollution control, which results in limited consideration of the connection

^{*} Corresponding authors.E-mail addresses: wylfuture@163.com (W. Wang), wq11ab@163.com (Z. Cao).

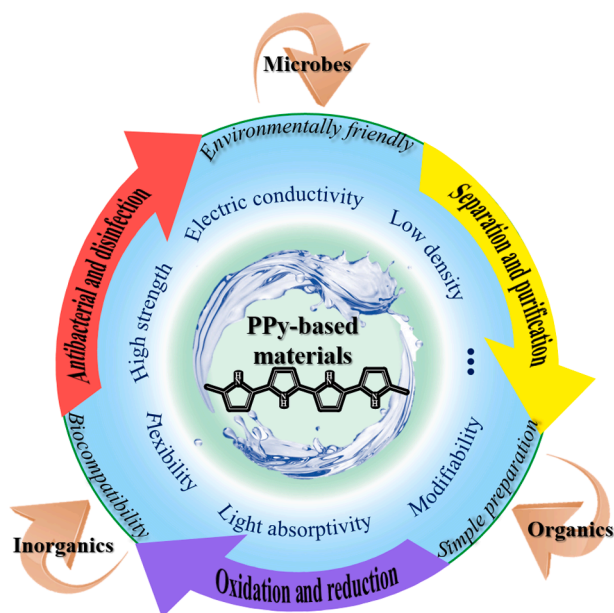


Fig. 1. Properties of PPy-based materials and their application in water pollution control.

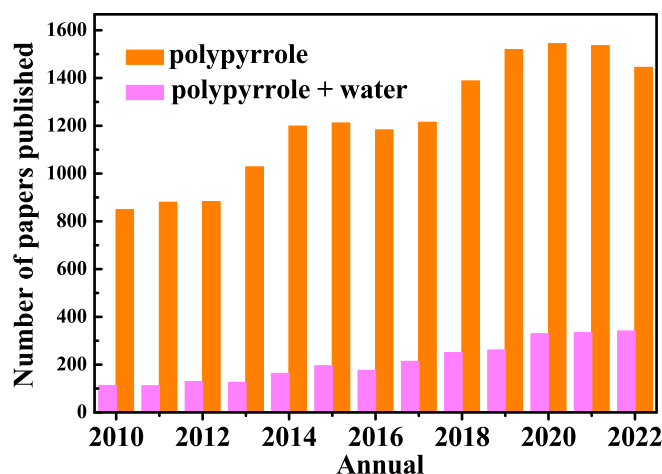


Fig. 2. Annual number of articles on the keywords “polypyrrole” and “polypyrrole + water” in Web of Science.

between material modification and technological intersection. This work aims to summarize the research achievements of PPy-based materials in the field of water pollution control, categorize them by technology type and action mechanism, and clarify the connection and synergetic development between materials modification and technological application. Moreover, in addition to focusing on system performance, this review pays more attention to the design ideas, improvement strategies, and existing problems of the technology. Finally, based on the summary and analysis of existing research results, this review highlights the remaining challenges and potential future directions in the field of PPy-based materials for water pollution control.

2. Synthesis and modification strategy of polypyrrole

Pyrrole oxidative polymerization can be divided into two types, namely, chemical oxidative polymerization and photoelectric oxidative polymerization (Fig. 3a). Commonly used oxidants include iron chloride, silver nitrate, potassium iodate, perchloric acid and persulfate.

Photoelectric oxidative polymerization methods include gamma ray oxidation [12], UV photooxidation [13] and anodic oxidation [14]. In the process of oxidative polymerization, the pyrrole ring undergoes a one-electron loss to generate an active intermediate that undergoes repeated bonding, rearrangement, and deprotonation processes, ultimately forming PPy (Fig. 3a).

Regarding its optical properties, pyrrole monomer is a colorless oily liquid, and as its increasing oxidation degree, the color of the polymer changes from colorless to black. This color transition can be explained by the fact that as the polymerization degree increases, the energy levels between the lowest and highest occupied orbitals in the molecular orbitals become closer, thereby reducing the excitation energy and causing the light absorption to shift from short to long wavelengths. When the polymerization degree covers the entire visible light region, the material appears black (Fig. 3a).

For the electric properties of PPy, due to its large π conjugated structure, the delocalized π electrons on the double bond can migrate along the molecular chain, resulting in high electric conductivity. However, unlike its optical properties, the electric conductivity of polypyrrole is affected by many factors. Pang et al. compared various factors on the conductivity of PPy, and found that when peroxide occurred, PPy would lose its electric conductivity and charge. When FeCl_3 was used as oxidizing agent, and the ratio of oxidant to monomer is 2 ± 1 , PPy-based materials with excellent electrical conductivity can usually be obtained [21]. Moreover, doping can change the electronic structure of PPy and induce electron delocalization [22].

Direct polymerization of pyrrole suffers from drawbacks such as particle agglomeration and low yield. To overcome these limitations, the template method has been employed to coat PPy on nanomaterials with different sizes, morphologies, structures, and physicochemical properties, resulting in high-performance PPy composite materials (Fig. 3b) [23,24]. In addition, both electrodeposition and interfacial polymerization can obtain PPy films, and membrane materials with different properties can be obtained by adjusting polymerization conditions [16,20].

The molecular structure of PPy can be modified by the following three means (Fig. 3c): 1) The secondary amino protonation of pyrrole is positively charged under acidic conditions. Anion doping (protonic acid, organic acid, etc.) can be used to introduce anions or other functional groups on the molecular chain of PPy, thereby improving the conductivity and activity of PPy [25]; 2) Copolymerization doping (polyaniline, polydopamine, etc.) can reduce the electron migration barrier while introducing other material characteristics, thereby enhancing the physical and chemical properties of PPy [26]. This technology is mostly used in energy, medical and other fine processing fields [27,28]; 3) In addition to improving the properties of PPy and its composite materials during the preparation process, the synthesized PPy material contains active amino groups that can be modified on the surface to alter the physicochemical properties of PPy and its composite materials [29,30].

3. Technologies for polypyrrole in water pollution control

In a variety of water pollution treatment technologies, the excellent usability and environmental coordination of materials are the most concerned. The properties and modifiability of PPy greatly expand its application scope and research content, and it is often used as the main body and medium in various water treatment technologies. In this section, the application fields and action mechanism of PPy are analyzed in detail from the separation and purification technology, oxidation and reduction technology, antibacterial and disinfection technology.

3.1. Separation and purification technology

3.1.1. Adsorption technology

Adsorption of organics: PPy has good adsorption performance for a variety of organic pollutants, such as organic dyes, drugs, oil pollution,

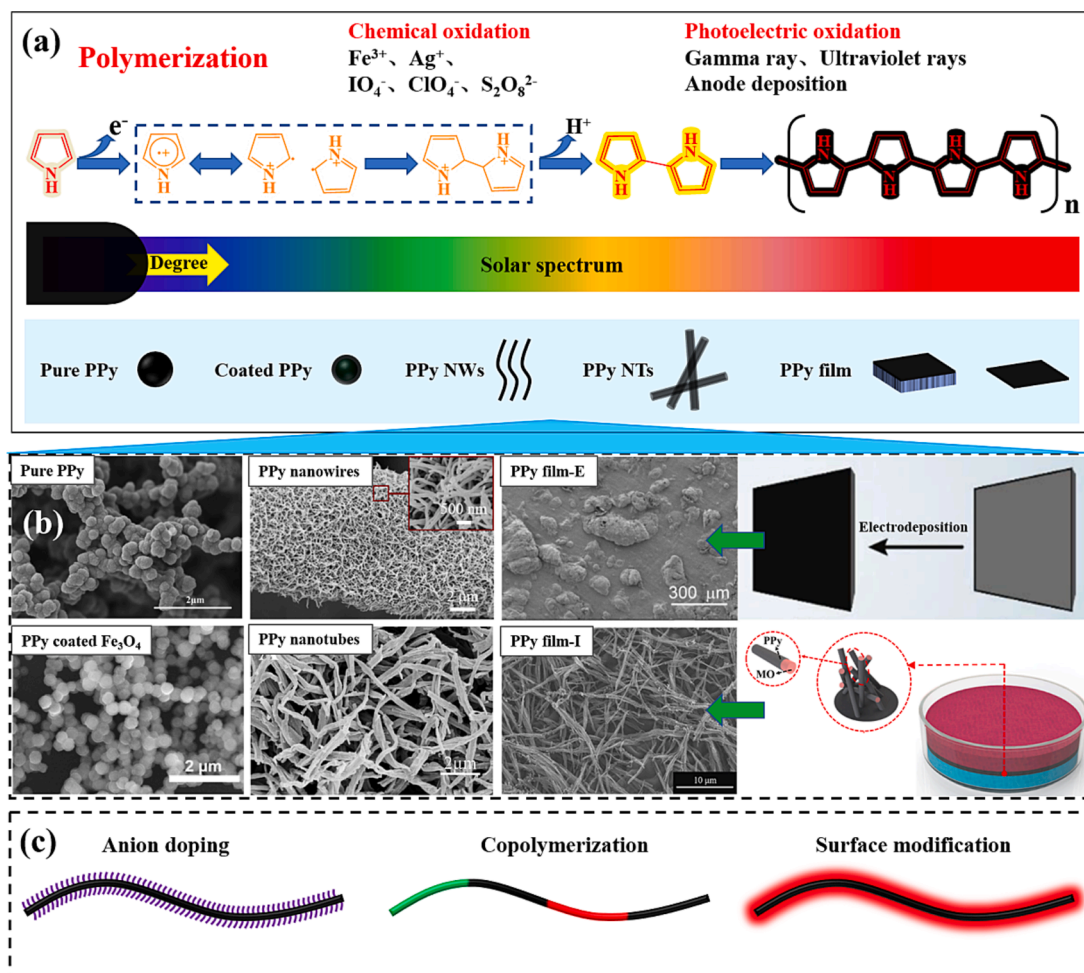


Fig. 3. Synthesis and modification strategy of PPy, (a) synthesis process and optical characteristics of PPy; (b) microstructure of various types of PPy [Reprinted with permission from Ref. [15–20]. Copyright, The Royal Society of Chemistry, American Chemical Society, and Elsevier]; (c) molecular structure modification strategy of PPy.

etc. [17,31–33]. To overcome the limitations of direct oxidative polymerization of pyrrole, collaborative preparation of PPy with other environmental functional materials through heterogeneous nucleation technology has been proposed to significantly increase its active area and adsorption capacity [34]. Furthermore, anionic doping has been applied to modify the zeta potential of PPy-based materials, and introduce new functional groups to increase interaction sites, thereby enhancing their structural affinity and chemical reactivity towards pollutants. Some of the reported doping substances include p-methylbenzenesulfonic acid, carboxymethyl cellulose, cyclodextrin mercaptan, and 4-vinylpyridine, among others [24,35]. Additionally, surface modification of PPy with organic acids can lead to the development of superhydrophobic materials, which have potential application prospects for oil–water separation (Fig. 4a) [29]. Moreover, because pyrrole can polymerize on the surface of a variety of materials and in environmental media, it provides many possibilities for the morphological structure of its composite materials, such as the preparation of hydrogel and aerogel materials, which meets the storage and recovery requirements of adsorbent materials [36,37].

Considering the molecular and electronic structures of adsorbates and adsorbents, the adsorption force of PPy based materials is mainly electrostatic interaction, hydrogen bonding, π - π conjugation, void filling, etc. (Fig. 4b). Among them, the electrostatic action and π - π conjugation action are the main forces.

The adsorption and desorption process of PPy (FeCl_3 as oxidant) on organic matter is shown in Fig. 4c. Under acidic conditions, PPy

protonation and electrostatically adsorbs Cl^- in water, and then negatively charged organics are adsorbed on PPy through ion exchange. Under alkaline conditions, PPy deprotonation leads to desorption of adsorbed organics. For the electronically controlled PPy adsorption and desorption behavior, the process is described as follows: under positive potential (oxidation state), PPy is protonation and thus has positive charge, the negative pollutants can be absorbed through anion exchange; Under negative potential (reduced state), PPy deprotonation, leading to the resolution of adsorbed pollutants (Fig. 4d) [38].

To better understand the adsorption process, the dominant adsorption force can be determined by the surface static charge distribution, electron density and differential charge density. Chen et al. studied the adsorption and removal of tetracycline by PPy/CMC aerogels, and the results showed that tetracycline removal efficiency was good in the range of $\text{pH} = 4$ –10, suggesting that electrostatic adsorption (sensitive to pH) was not the main adsorption process. According to electrostatic potential and electron density analysis, π - π -electron donor–acceptor interaction has great affinity for tetracycline and is the main adsorption force (Fig. 4e) [37].

The above mechanism studies show that PPy adsorbent has a good adsorption effect on substances containing benzene rings, heteroatoms and negative charges. However, functional group modification can alter the surface electrical properties of composite materials, thereby expanding the adsorption range of organic compounds, realizing the adsorption and removal of different charged organic pollutants. Therefore, PPy can be modified purposefully according to the molecular

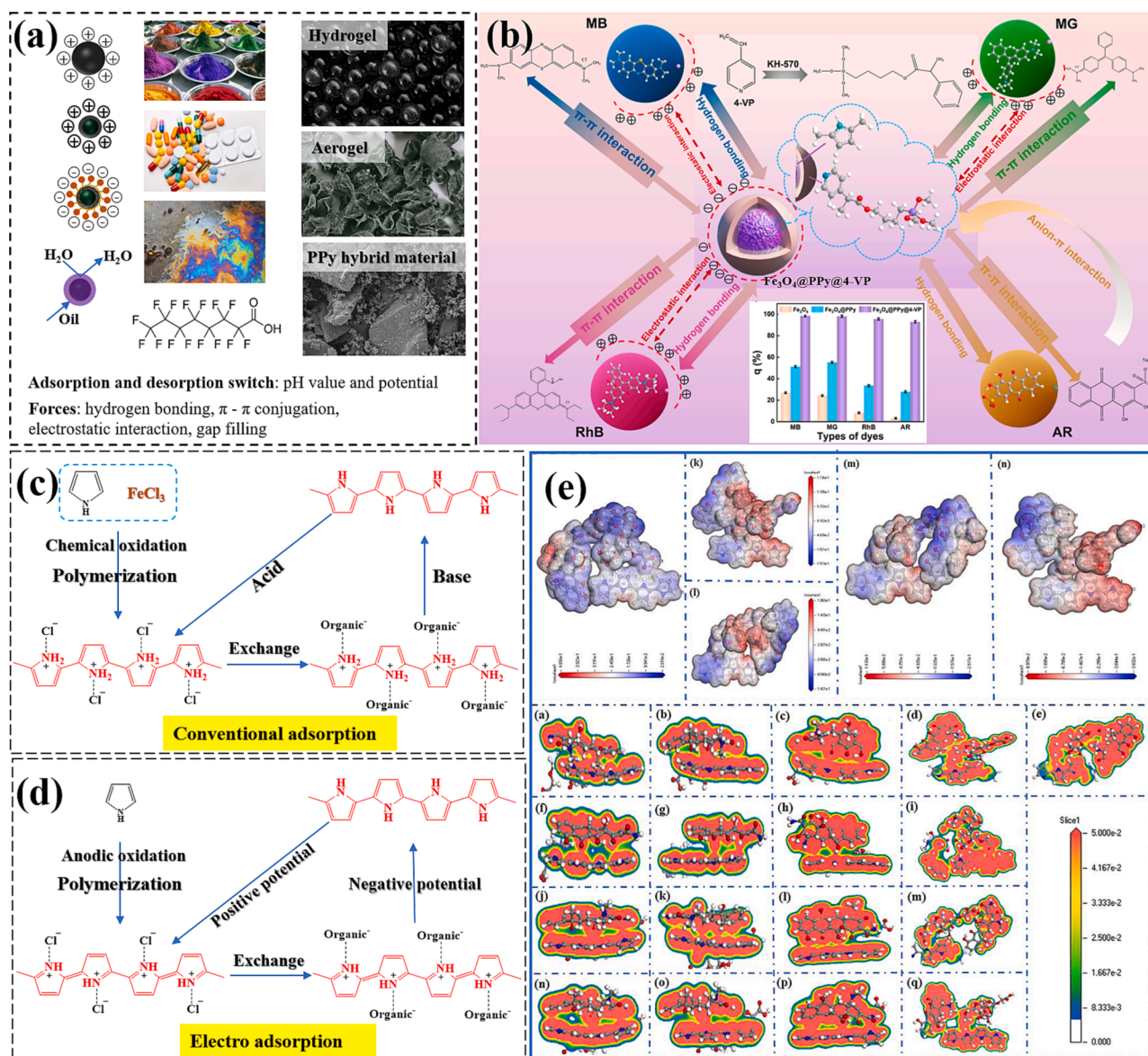


Fig. 4. (a) Modification of PPy material and its application range; (b) Adsorption effect and mechanism diagram of PPy matrix composites on different organic dyes [Reprinted with permission from Ref. [19]. Copyright 2022, American Chemical Society]; (c) Adjusting the adsorption and desorption process of PPy on organic matter through pH changes; (d) Adjusting the adsorption and desorption process of PPy on organic matter through potential changes; (e) Electrostatic potential diagram and electron charge density images for tetracycline adsorbed on PPy/CMC aerogels [Reprinted with permission from Ref. [37]. Copyright 2023, Elsevier].

structure of pollutants. The adsorption conditions can be optimized according to the isoelectric point of PPy based composites, and the adsorption and desorption process of organic compounds can be regulated through changes in pH value and potential.

Adsorption of inorganic ions: Inorganic ions mainly high valence oxyacid radicals (MnO_4^- , $\text{Cr}_2\text{O}_7^{2-}$, ClO_4^- , SO_4^{2-} , NO_3^-), halide ions, heavy metal ions, and radionuclide. All of them have significant negative impacts on the ecological environment and human health [30,39,40]. PPy-based adsorption materials mainly remove the above-mentioned pollutants through electrostatic action, but different treatment processes have been developed due to differences in the physical and chemical properties of the pollutants.

Take Cr(VI) adsorption-reduction as an example. By report, the adsorption capacity was well-correlated with the pyrrolic nitrogen exposure concentration [41]. Coating PPy on nanomaterials can increase the number of exposed adsorption sites, achieving higher adsorption capacity than nanomaterial substrates and PPy monomers (Fig. 5a) [42]. In addition, the pH value will have an impact on the form

of pollutants (Fig. 5b) and the adsorption force. When the pH value of the solution is less than the zero charge point on the adsorbent surface, the N atom is protonation, which can electrostatic adsorb high valence oxyacid radicals in water (Fig. 5c) [43]. Based on these, high valence oxyacid radicals in water are usually removed under acidic conditions ($\text{pH} < 4$). The removal mechanism of PPy on Cr(VI) is as follows (Fig. 5d) [44]:

- (1) Formation of protonated nitrogen and introduction of counter anions in PPy under acidic conditions
- (2) The counter anions are replaced by Cr(VI) anions via ion exchange;
- (3) On the electron rich PPy surface, Cr(VI) is reduced to Cr(III) through an amino reaction (from secondary amine to tertiary amine);
- (4) The desorption process of adsorbed Cr(III) under alkaline conditions.

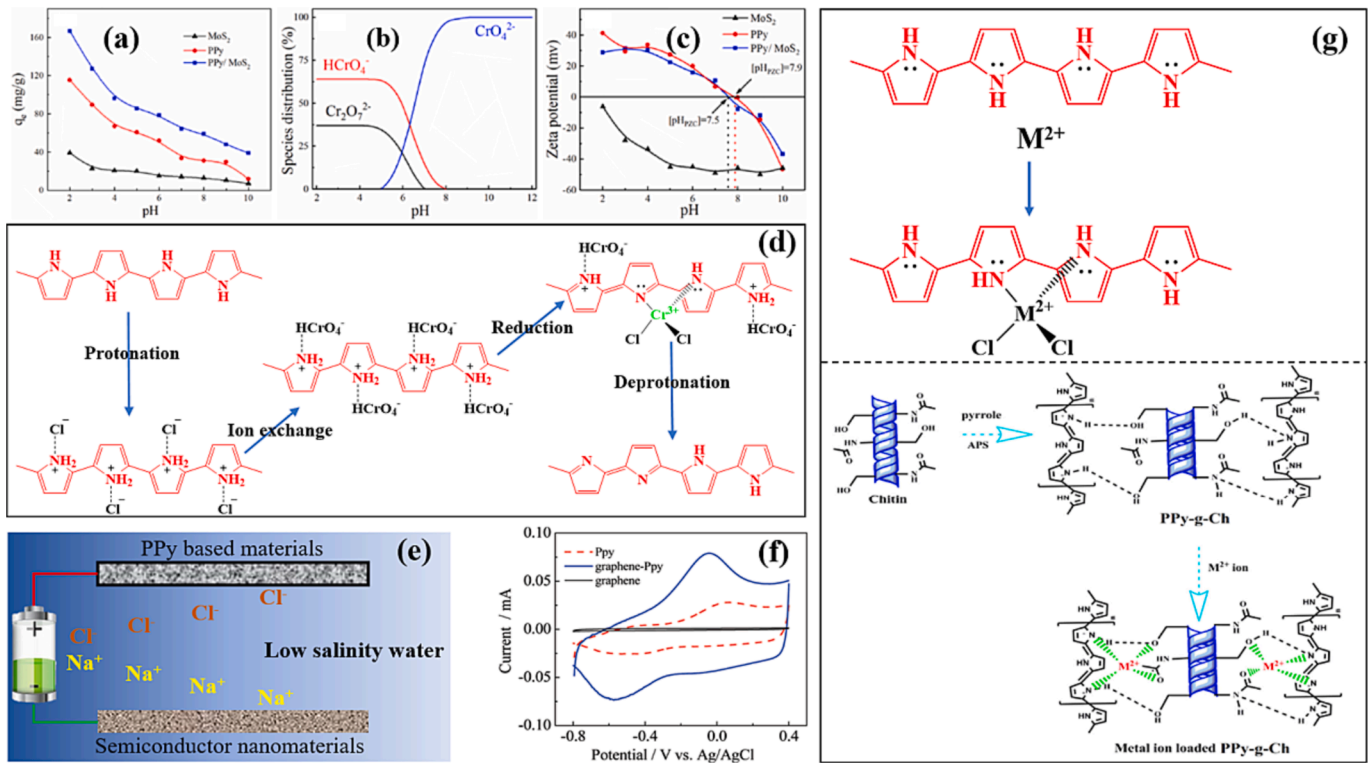


Fig. 5. (a) Changes in the adsorption ratio of Cr (VI) before and after PPy coating of nanomaterials; (b) Species distribution of Cr(VI) as a function of pH; (c) Zeta potentials of MoS_2 , PPy and PPy/ MoS_2 [Reprinted with permission from Ref. [42]. Copyright 2021, Elsevier]; (d) Adsorption-reduction process of Cr (VI) on PPy; (e) Schematic diagram of capacitive deionization; (f) Determination of adsorption capacity of PPy based materials [Reprinted with permission from Ref. [45]. Copyright 2011, American Chemical Society]; (g) PPy adsorbs heavy metals (up), collaborative removal of heavy metals in water using PPy-chitosan composite material (down) [Reprinted with permission from Ref. [46]. Copyright 2015, Elsevier].

Table 1

The adsorption performance of different adsorption materials for Cr (VI) in water.

Material	C_0 (mg/L)	T (K)	pH	q_e (mg/g)	Dynamic	Isotherms	Ref.
CPM/PDA/PPy	100	298	2	262.33	pseudo-second-order	Langmuir	[47]
PPy/ MoS_2 /PPy	120,150	298	2	257.73151.29	pseudo-second-order	Langmuir	[42]
PPy nanotube	150	298	2	250.31	pseudo-second-order	Langmuir	[20]
PPy/CB	100	298	3	211.10	pseudo-second-order	Langmuir	[41]
PPy/ Fe_3O_4	200	298	2	208.77	pseudo-second-order	Langmuir	[48]
PPy/ Fe_3O_4 /rGO	250	303	3	226.8	pseudo-second-order	Langmuir	[49]
PPy/calcium rectorite	100	298	1.5	100.91	pseudo-second-order	Langmuir	[50]
PAN/PPy	200	298	2	61.8	pseudo-second-order	Langmuir	[51]
Calcined PANI/LDOs	120	293	2	409.77	pseudo-second-order	Langmuir	[52]
Iron-clay biochar	100	298	2	91.13	pseudo-second-order	Langmuir	[53]
FeS/HTs	300	298	3	206.2	pseudo-second-order	Langmuir	[54]
NH_2 -graphene sponge	165	298	1	166.46	pseudo-second-order	Langmuir	[55]
Magnetic hydrogel beads	400	298	2	342.5	pseudo-second-order	Langmuir	[56]
N,S-C/ Fe_3O_4	100	303	5	134	pseudo-second-order	Langmuir	[57]
MNC@PmPD	100	303	2	159.23	pseudo-second-order	Langmuir	[58]

CPM: carbon protective mask; CB: carbon black; PDA: polydopamine; PANI: polyaniline; LDOs: Mg-Al layered double oxides; HTs: hydrotalcites; MNC: magnetic nanoporous carbon; PmPD: Poly(m-phenylenediamine).

As a comparison, the adsorption performance of PPy based adsorbents and other adsorbents for Cr (VI) is shown in Table 1. According to the adsorption kinetics and adsorption isotherm, Cr (VI) removal conforms to the single-layer chemical adsorption model, and its adsorption process is determined by both surface adsorption and internal diffusion.

F^- has strong dissociation, and PPy alone has limited adsorption capacity for F^- . By combining with metal matrix materials, good adsorption and removal effects can be achieved for F^- [59]. For example, Chen et al. prepared PPy/ TiO_2 for adsorption and removal of F^- , the adsorption was mainly carried out through electrostatic attraction, and also involved ion exchange and chelation. Hydroxyl groups (ion exchange) and positively charged nitrogen atoms (electrostatic

adsorption) played important roles in adsorption. The maximum adsorption capacity was 33.178 mg/g, which was 5 times that of pure PPy [60]. In addition, the removal of F^- from water can be further enhanced by electro adsorption technology. Kang et al. prepared PPy films on graphite substrates by electrodeposition, and then electrophoretic deposition of metal organic skeleton Ce/Zn BDC- NH_2 (CZBN) on the PPy films, the removal ratio of F^- can reach 55.12 mg/g. Mechanism studies have shown that the metal organic skeleton was the main adsorbent in this process, and PPy mainly acted as a conductive intermediate layer [16].

Cl^- generally exists in high salt wastewater and seawater, conventional adsorption techniques are not suitable for the removal of such a

Table 2

Membrane parameters before and after PPy modified PVDF.

Membrane type	Pore size distribution	Water pressure	Water flux (L/m ² /h ¹)	Contact angle	Environment
PVDF	72–101 nm	1 bar	203.08	79.61	
PPy-DBS/PVDF	70–88 nm	1 bar	170.43	25.28	oxidation
			158.02		standard
			134.16		reduction

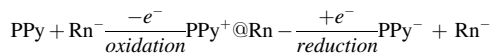
DBS: Dodecylbenzene sulfonate.

large amount of Cl^- . Based on efficient engineering applications, electrically driven Cl^- adsorption (pseudocapacitive deionization) has attracted much attention, which is implemented by using PPy and its composite materials as anodes and metal compounds (such as MnO_2 , iron hexacyanoferrate, etc.) as cathodes [61,62]. Under the action of an external electric field, Na^+ and Cl^- tend towards the anode and cathode respectively, when the direction of the external electric field changes, Na^+ and Cl^- desorb from the electrode and enter the aqueous solution (Fig. 5e) [63]. Notably, the active area of the anode is not positively correlated with the amount of PPy coating and the specific surface area of the anode material, and attention should be paid to the microstructure design of the anode material [64,65]. Through the cyclic voltammetry curve, the adsorption capacity of the PPy based material can be intuitively observed, which can predict the advantages and disadvantages of adsorbents (Fig. 5f) [45].

The main adsorption sites of heavy metal ions in PPy based adsorbents are nitrogen atoms in the macromolecular chain, so the protonation process of PPy is not beneficial to the adsorption and removal of heavy metals. In order to achieve high removal of heavy metal ions, the optimal pH value of adsorption is theoretically higher than the isoelectric point of PPy based adsorption materials. Since the lone pair of electrons of pyrrolidine nitrogen participate in π - π conjugation, deprotonation PPy can effectively combine with metal ions to form metal complexes (Fig. 5g) [66,67]. In addition, PPy modified by functional groups or compounded with other electronegativity materials (chitosan, bentonite, etc.) can change the apparent electrical properties of coupling materials, so as to achieve the excellent adsorption and

removal of heavy metals [46].

Radionuclides (Rn) can spontaneously emit radiation (α -ray, β -ray, etc.), is a kind of carcinogen. Electrochemically switched ion exchange technique, the reversible adsorption and desorption of the target ions can be controlled by changing the redox state of working electrode. In existing research, ReO_4^- and I^- were respectively used as substitutes for $^{99}\text{TcO}_4^-$ and I^{131} , and carbon materials were used as the substrate for electro oxidation deposition of PPy film. This system can control the uptake (positive potential) and release (negative potential) of electro-negativity radionuclides (Rn^-) by adjusting the potential. The adsorption performance and electrochemical reaction of materials were judged by CV curve, and the adsorption occurrence and binding type were determined by combining with XPS. The carbon electrode modified with PPy had good adsorption and desorption performance, recycling performance, and selectivity [68,69]. The action process is as follows:



Correspondingly, for positively charged Rn (Rn^+), PPy modified electrode can achieve uptake at negative potential and release at positive potential. As report, electrodeposition of PPy on the BC surface can effectively separate and purify U(VI) in radioactive wastewater by electroadsorption. The maximum adsorption amount of UO_2^{2+} in the electrode with graded porous structure was 237.9 mg/g [70].



3.1.2. Membrane technology

Ultra/Nano-filtration membranes: Membrane fouling causes serious membrane flux attenuation and increased water treatment costs. How to reduce or avoid membrane fouling is directly related to the application prospects of membrane technology. Research has found that PPy undergoes reversible volume changes during the redox process due to ion doping and dedoping behavior. The unique properties of PPy provide the possibility of intelligent switching between microporous mode (filtration process) and macroporous mode (backwashing process) [71]. As shown in Table 2, after PPy modification of PVDF membrane, the pore size distribution, contact angle, and water flux of the membrane all changed. Especially in the oxidized state, PPy-DBS/PVDF had a

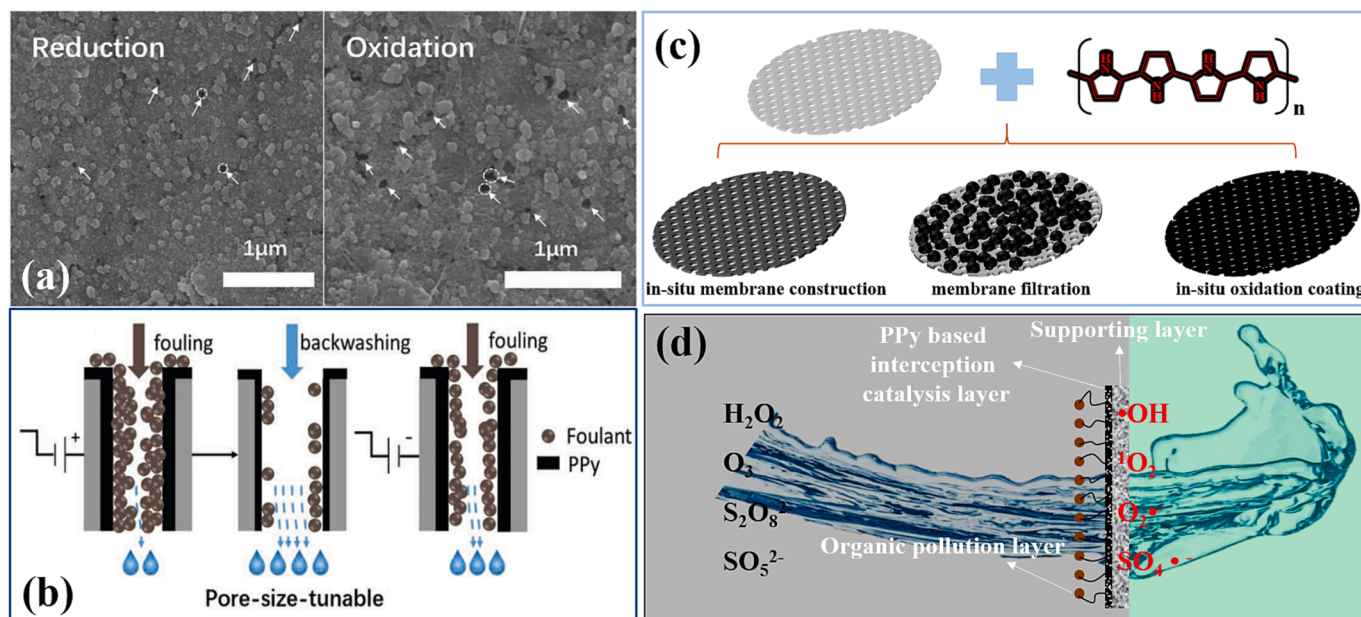


Fig. 6. (a) SEM images of oxidized and reduced PPy-DBS/PVDF membranes, (b) schematic diagram of water permutation for PPy-DBS/PVDF membrane in the presence of applied voltages [Reprinted with permission from Ref. [71]. Copyright 2019, Wiley-VCH Verlag]; (c) PPy coupled nanofiltration membrane methods; (d) Advanced oxidation coupled membrane filtration technology.

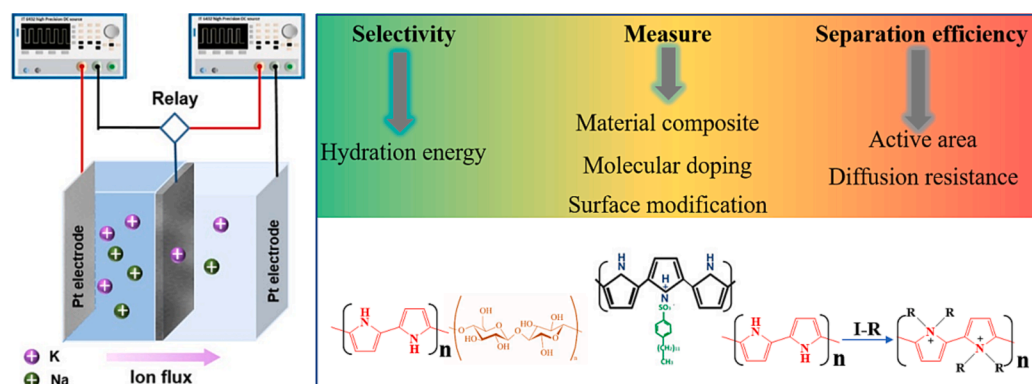


Fig. 7. Cation exchange technology participated by PPy (left) and membrane material design concept (right) [Reprinted with permission from Ref. [75–77]. Copyright, Elsevier and American Chemical Society].

greater water flux, indicating that the membrane pore size was larger in the oxidized state than that of the reduced state (Fig. 6a). Overall, the results proved that the pore size of the PPy-DBS membrane was dynamically regulated by the voltages, and combined with backwashing could effectively relieve membrane fouling (Fig. 6b).

For nano-filtration membranes, three ways were used to introduce PPy into membranes: in-situ membrane construction, membrane filtration, and in-situ oxidation coating (Fig. 6c). Thanks to the good material compatibility, adsorption ability and corrosion resistance of PPy, it can significantly improve the retention rate, water flux, and mechanical stability of the nano-filtration membrane [72,73]. Meanwhile, PPy was also often combined with carbon materials to improve nano-filtration membrane performances [13]. Moreover, the synergy of advanced oxidation process and membrane separation technology can effectively remove organics in wastewater and mitigate membrane fouling. Carbon materials are environmentally friendly materials that catalyze the generation of active radicals. By organically combining PPy with carbon materials, an excellent electron transfer system can be constructed. Xu et al. constructed a CNT-PPy/PVDF membrane electroactive

peroxydisulfate system, in which the filtration membrane had three major functions: mitigating membrane fouling, activated persulfate, and antioxidant, effectively improving the removal efficiency of organic pollutants in water (Fig. 6d) [74].

Cation exchange membranes: Cation exchange membranes are of great significance in strategic metal extraction and high salinity desalination treatment. The secondary amino groups and electronic properties of PPy molecules form the basis for their cation selection and rejection, therefore widely used in the research of cation exchange membranes. Researches have shown that material composition, molecular doping, and surface modification can all affect the selectivity, separation efficiency, and energy consumption of PPy based cation exchange membranes (Fig. 7). For example, PPy-CTS modified cation exchange membrane had a larger electroactive area and better electric conductivity, resulting in a higher ion exchange capacity (1.04 mM/L) and a threefold increase in selectivity for monovalent ions (Na^+ vs Mg^{2+}) compared to the original membrane [75]; PPy membrane doped with sodium dodecyl benzene sulfonate molecule showed K^+ selectivity (K^+ / Na^+ separation factor is 2.10), and the energy consumption of

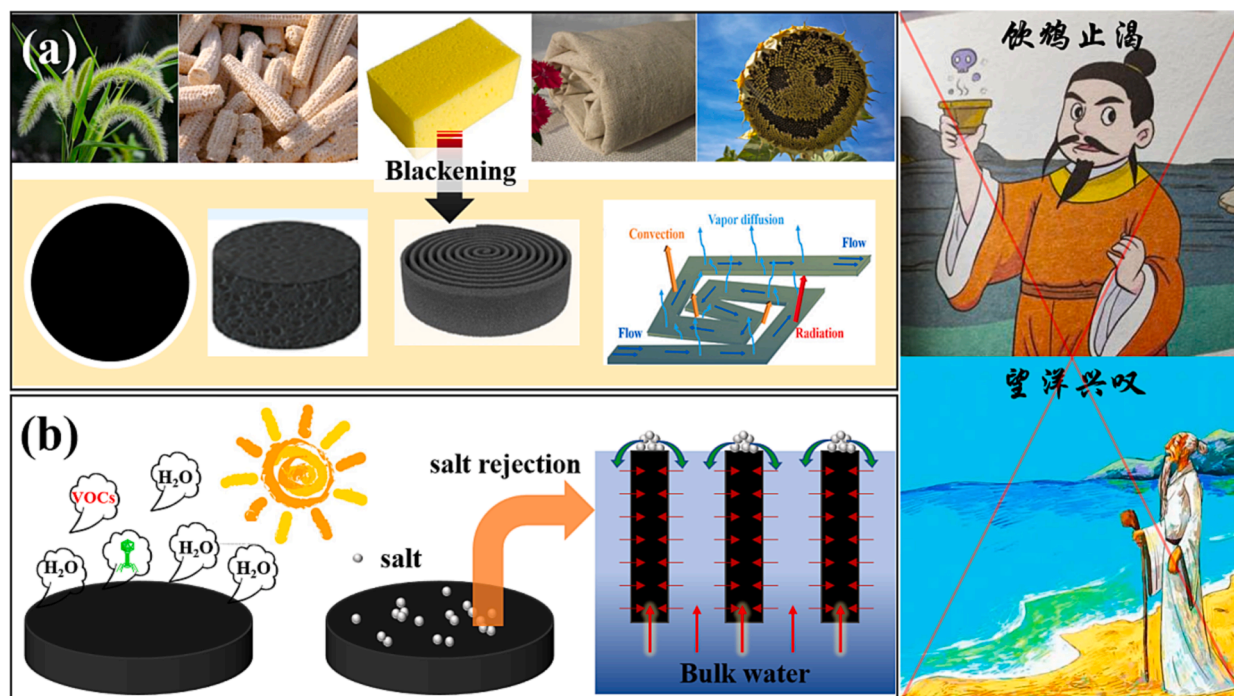


Fig. 8. (a) Selection and engineering design of water evaporator substrates [Reprinted with permission from Ref. [81,82]. Copyright 2020 and 2022, American Chemical Society]; (b) existing problems in photothermal water evaporation and solutions to some problems.

electrodialysis was 3.80 kWh/kg K, 37% lower than that of traditional electrodialysis [76]; Pang et al. modified PPy through hydrophobicity to increase the hydration energy of monovalent and divalent ions through the membrane. The $\text{Na}^+/\text{Mg}^{2+}$ permeation selectivity reached 21.93, and the Li/Mg permeation selectivity reached 1.71, which were 6.3 and 1.6 times higher than commercial membranes, respectively [77].

In summary, smaller hydration ionic radius generally has lower hydration energy, resulting in stronger separation efficiency of monovalent cations; The more hydrophobic the membrane is, the higher the Gibbs hydration energy required for cations to pass through the membrane, especially for high valence cations. The above description forms the basis for the permeation selectivity of membranes towards cations, and the order of cation selectivity flux is: $\text{K}^+ > \text{Na}^+ > \text{Li}^+ > \text{Mg}^{2+}$. To achieve higher separation efficiency of cations, it is necessary to design membrane materials with larger active area and lower diffusion resistance. How to balance ion selectivity and separation efficiency will be a long-term research topic in the future.

3.1.3. Photothermal techniques

Solar water evaporation technology organically unifies material science, structural engineering and fluid mechanics, and can effectively deal with high salt, heavy metal, acid, alkali, dye and other polluted water bodies [78]. Commonly used photothermal materials include metal nanoparticles, semiconductors, carbon materials, and polymers. Among them, PPy has a large conjugated structure, low thermal conductivity, and can well absorb solar radiation in both dry and wet conditions [79]. In addition, its good surface film-forming ability can easily achieve “blackening” of different structural substrates [80], making it a more ideal photothermal material compared to other materials (Fig. 8a).

Sewage purification: For high salt wastewater or refractory organic wastewater, solar water evaporation is an effective sewage purification technology. Thanks to research in structural engineering and fluid mechanics, the water evaporation rate of photothermal evaporator constructed by PPy is growing rapidly at present, and there has been a research report on the evaporation of $3.72 \text{ kg/m}^2/\text{h}^1$ [83]. Especially in the treatment of oily wastewater, surface modification of PPy coated films can obtain superhydrophilic photothermal surfaces and underwater superhydrophobic materials, effectively achieving anti oil fouling and continuous efficient water evaporation efficiency [84]. Nevertheless, there are still some challenges in using photothermal technology to achieve sewage purification. For example, volatile organic compounds (VOCs) can be condensed and recycled along with water vapor, resulting in poor treatment efficiency for wastewater containing VOCs [85,86]. It has been reported that the reduced graphite oxide/polypyrrole mixed aerogel can be used for photocatalytic purification and water evaporation at the same time, but in the experimental design, water evaporation and photodegradation were carried out separately, and the timeliness problem in practical application was not paid attention to [87]. In addition, due to the decrease in saturated vapor pressure of water in the evaporator, water can be vaporized below 50°C [88]. Therefore, the presence of pathogenic microorganisms in condensed water also requires attention, but there have been no relevant reports so far (Fig. 8b).

Seawater desalination: Seawater desalination is a promising technology to solve water resource shortages. The average salinity of seawater is 3.5%, and because the saturated vapor of salt water is lower than that of pure water, the evaporation rate of saline water is slightly lower than that of pure water. In addition, with the continuous generation of water vapor, salt precipitation is prone to occur on photothermal materials, thereby reducing the evaporation capacity of the evaporator. The current response measures include: 1) Constructing a dual scale capillary structure, where the salt generated by water evaporation on the surface of the photothermal material dissolves with the water flow between the material pores, resulting in good salt rejection performance of the water evaporator (Fig. 8b) [82,89]; 2) Combining the siphon effect to enhance the flow of water in the evaporator,

Table 3

Water evaporation efficiency of different photothermal materials and design characteristics of photothermal systems.

Material	Radiation intensity	Evaporation rate $\text{kg/m}^2/\text{h}^1$	Characteristic	Ref.
PPy + PVDF	1 sun irradiation	1.30	classic design	[18]
PPy + flax fabric	1 sun irradiation	1.40	salt-rejection	[89]
Modified-PPy + cotton	1 sun irradiation	1.54	anti-oil-fouling	[84]
Ag/PPy + substrate	1 sun irradiation	1.55	antibacterial film	[90]
PPy + PVDF roll	1 sun irradiation	1.93	2D → 3D, salt-rejection	[82]
PPy-FexOy-CTS hydrogel	1 sun irradiation	1.93	Gel coating process	[85]
rGO/PPy aerogel	1 sun irradiation	2.08	photooxidative degradation	[87]
PPy + MXene + sponge	1 sun irradiation	2.45	siphon and zigzag-shaped device	[81]
PPy + maize straw	1 sun irradiation	3.00	obtain raw material locally	[91]
PPy + PVA hydrogel	1 sun irradiation	3.20	3D Hydrogel	[92]
PPy + Setaria viridis Spike	1 sun irradiation	3.72	obtain raw material locally	[83]
MXene	1 sun irradiation	≈ 1.00	suction filtration	[93]
Ag/diatomite	1 sun irradiation	≈ 1.39	suction filtration	[94]
GO thin film	0.82 sun illumination	2.00	dip-coated	[95]
rGO + PVA hydrogel	1 sun irradiation	2.50	mix	[96]
Craphene nanosheets	1 sun irradiation	2.67	3D printing technology	[97]

allowing the precipitated salt to dissolve again with the water flow [81].

Compared with metals, semiconductors, and carbon nanomaterials, the research of PPy as a photothermal material is relatively late, but it is highly favored due to its excellent light absorption ability and film forming properties. In Table 3, it can be seen that the introduction of PPy greatly enriches the design scheme of water evaporators and promotes the improvement of water evaporation rate, compared to other photothermal materials, the introduction of PPy has realized the possibility of multiple structural design of the water evaporator (corn cob, sunflower plate, pennisetum, aerogel, hydrogel), and removed the obstacles to the improvement of water evaporation from the material structure level. Admittedly, PPy is the best choice for photothermal materials at present, and the limitations of photothermal technology have shifted from the selection of photothermal materials to the backwardness of engineering technology. How to achieve VOCs removal and sterilization in wastewater is a problem that needs to be considered at present.

3.2. Oxidation and reduction technology

3.2.1. Oxidation technology

Photooxidation: Compared to UV photocatalysis, visible photocatalysis has more practical application prospects. PPy can generate photogenerated electrons and holes in almost the entire visible light spectral range. Meanwhile, PPy has excellent electronic and photo-physical properties of inorganic semiconductors, as well as the advantages of easy molding and low cost of organic materials. Li et al. compared the photocatalytic performance of P25, g-C₃N₄, and PPy materials, and found that PPy exhibited excellent photocatalytic performance in the degradation of organic pollutants under full spectrum and visible light. The calculated band gap of PPy was 2.12 eV (excitation wavelength approximately 585 nm), indicating that the orbital electron

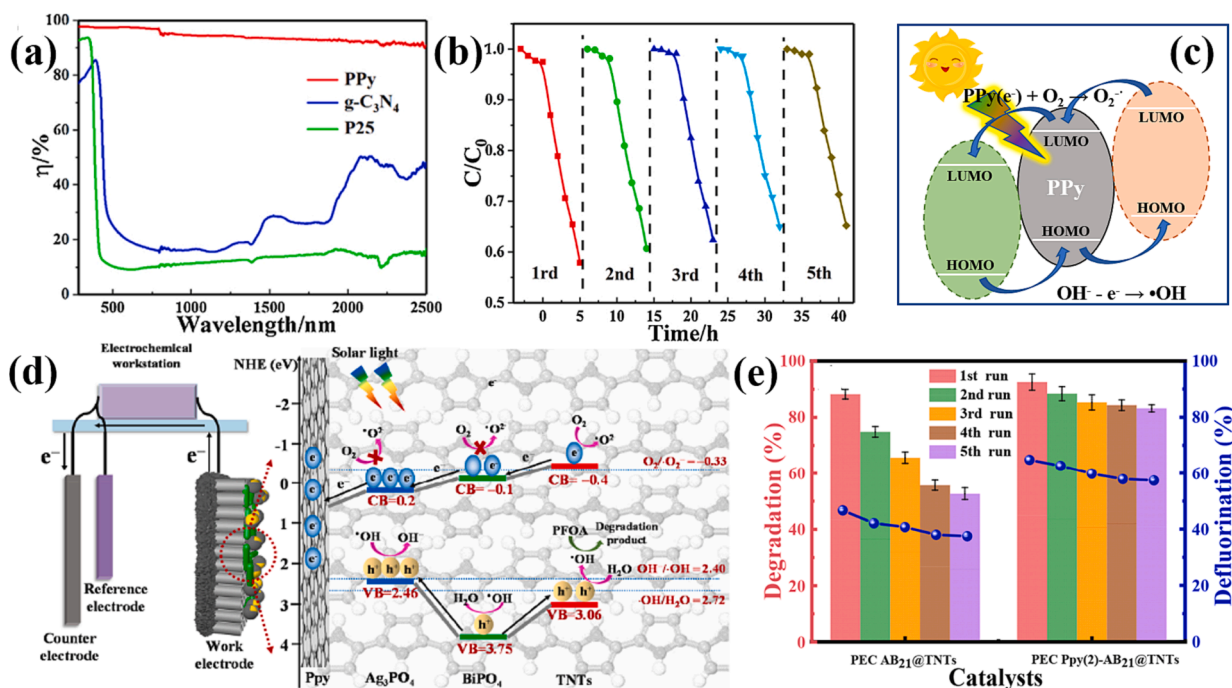


Fig. 9. (a) Light response intensity of PPy, g-C₃N₄, P25 [Reprinted with permission from Ref. [98]. Copyright 2021, Elsevier]; (b) Cycling experiments for the degradation of MO over PPy under full spectrum light [Reprinted with permission from Ref. [98]. Copyright 2021, Elsevier]; (c) Degradation mechanism of PPy coupled with other photocatalysts; (d) The photoelectrooxidation mechanism involved in PPy [Reprinted with permission from Ref. [99]. Copyright 2021, Elsevier]; (e) Cyclic performance for the photoelectric degradation of PFOA [Reprinted with permission from Ref [99]. Copyright 2022, Elsevier].

transitions of PPy can be excited in visible light except for red and orange light. Mechanism research found that superoxide radicals played an important role in pollutant degradation (Fig. 9a). The study on the fatigue resistance found that PPy showed good structural stability during degrading organic pollutants by photooxidation (Fig. 9b), and the slight decrease in activity was attributed to material loss during repeated use. In addition, the results of instrument analysis showed that the FT-IR, SEM and XRD characteristics of the materials before and after the reaction were not significantly different [98].

Based on the excellent photosensitivity and stability of PPy, it is often used to composite with traditional semiconductor materials (carbon quantum dots [100], TiO₂ [101], ZnO [102], MoSe₂ [103], Ag₃PO₄ [104] etc.) to enhance the photocatalytic degradation performance of pollutants. The introduction of PPy can improve the response to visible light, and act as an effective electron donor and a suitable hole medium, thus accelerating the separation of electron hole pairs and reducing the photo corrosion of catalysts (Fig. 9c). The heterogeneous structure has been widely used in the oxidation treatment of dye wastewater, phenol wastewater and oil wastewater [105,106].

Furthermore, Zhang et al. prepared PPy-Ag₃PO₄/BiPO₄ TNT photoelectrodes and used them for the photoelectric degradation of PFOA (Fig. 9d) [99]. The experimental data showed that PFOA may be degraded by both hole oxidation and electron reduction, the removal ratio of 100 mg/L PFOA reached 92.5% and defluorination ratio was 64.8% after 3.0 h under simulated sunlight and biased potential of 2.0 V (vs. Ag/AgCl). The presence of PPy can cause strong interactions between Ag₃PO₄ and BiPO₄, accelerate the separation of electron hole pairs, and inhibit the photo corrosion of Ag₃PO₄. The application of bias potential can enhance degradation performance through more effective electron transfer. In addition, due to the introduction of PPy, the reuse performance of composite materials had also been significantly enhanced (Fig. 9e) [99].

Electrooxidation: The potential of anodic oxidation to obtain PPy films is generally below 1.0 V. If PPy-based composite materials are directly used as anodes, it is prone to problems such as oxygen evolution

side reactions and PPy membrane separation. Therefore, there are almost no reports of PPy being used as anodes to directly degrade pollutants in water. However, PPy can be used to modify the cathode to build an electric Fenton catalytic system. Zhang et al. prepared a novel 3D anthraquinone/polypyrrole modified metal catalyst, and then it was used to catalyze the oxygen generated on anode into H₂O₂, which can generate a large number of superoxide free radicals with the participation of Fe²⁺. Among them, PPy modified cathode promoted the production of H₂O₂ and accelerated the catalytic cycle of Fe²⁺/Fe³⁺, thus realizing the rapid degradation of organic matter in water. After repeated use for 10 times, the degradation rate of pollutants was still more than 90%, showing good reuse performance [107].

Chemical Oxidation: The N heteroatom in PPy can activate the inert carbon skeleton by increasing the charge density of adjacent carbon atoms, thus promoting the interaction between the catalyst and PS. Ait El Fakir et al. prepared PPy monomer and its hydrogel spheres to activate PS to effectively degrade orange G. Experimental research found that although the hydrogel reduced the catalytic activity of PPy, its stability and repeatability were significantly improved, the active species were detected as SO₄•⁻, •OH and ¹O₂ [108].

Compared to metal based catalysts, PPy has poor catalytic oxidation activity. Currently, it is mainly combined with metal based catalysts to achieve synergistic interaction. Zhang et al. used PPy to encapsulate Pd/Fe₃O₄ and degraded RhB through Fenton reaction, achieving good catalytic effect and catalyst recovery repeatability. Experiments confirmed that the thin PPy shell can effectively avoid the erosion of active components and will not weaken the catalytic activity [109]. Chen et al. studied the Fenton degradation of p-nitrophenol by rGO/PPy/nZVI. rGO/PPy stabilized nZVI by forming electron transfer complexes, accelerated the decomposition of H₂O₂ into free •OH, and promoted the redox cycle of Fe(III)/Fe(II) through the electron donating ability of rGO/PPy [110]. In addition, Ali et al. used PPy-zirconium selenoiodate cation exchange nanocomposites to immobilize ginger peroxidase and activate H₂O₂ through strong electrostatic interactions to degrade methyl violet 6B wastewater. The experimental results showed that PPy

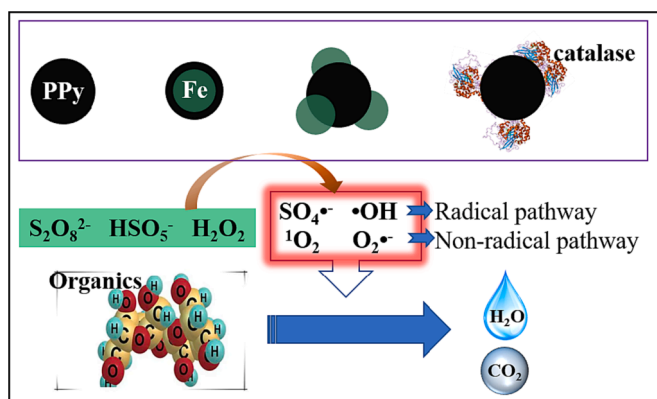


Fig. 10. Application of PPy on degradation of organic pollutants in water by chemical oxidation technology.

assisted in enhancing the electron shuttle system of the enzyme, improving its activity and stability [111]. A brief summary of the above reports is shown in Fig. 10.

3.2.2. Reduction technology

Photoreduction: PPy is a p-type semiconductor with hole carriers, indicating that it is conducive to photocatalytic oxidation and not conducive to photocatalytic reduction. Therefore, there are few reports on the direct use of PPy for photoreduction systems. The preparation of heterogeneous photocatalysts by combining PPy with other photocatalysts is a good solution to the above problems. Abinaya et al. prepared excellent visible light catalysts by binding PPy with Ag_2MoO_4 , which can achieve the reduction of Cr(VI) in water in a short time (<10 min) (Fig. 11a). Moreover, this system showed good repeatability (Fig. 11b)[112]. Cheng et al. constructed $\text{Fe}_3\text{O}_4@\text{SiO}_2@\text{PPy}$ (semiconductor insulator semiconductor) heterostructure, unlike PPy alone, when Fe_3O_4 , SiO_2 , and PPy were combined into a ternary heterostructure, the photoelectric properties of PPy underwent a reverse change. The majority of charge carriers on the surface of PPy were converted into photoelectrons, and the SiO_2 (insulator) layer (1–2 nm) can effectively prevent the recombination of photo generated hole electron pairs. At the same time, a few charge carriers were “pushed” in the opposite direction through the electrostatic field, further playing a dominant role in the photoreaction process (Fig. 11c-d). After 90 min of photoreaction, the removal rate of Cr(VI) reached 99.2% [113].

[Reprinted with permission from Ref. [112]. Copyright 2019, American Chemical Society]; (c) Mechanism diagram of Cr(VI)

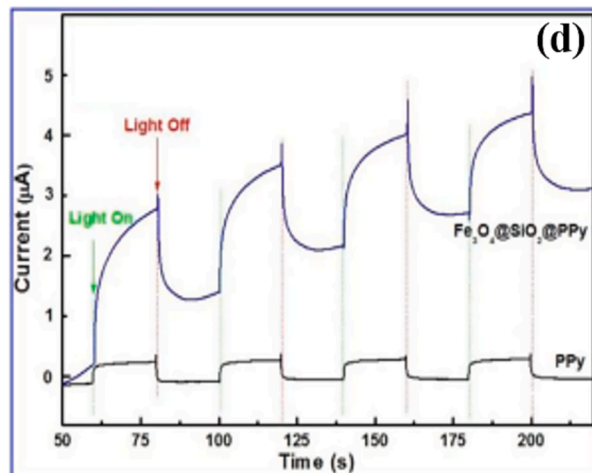
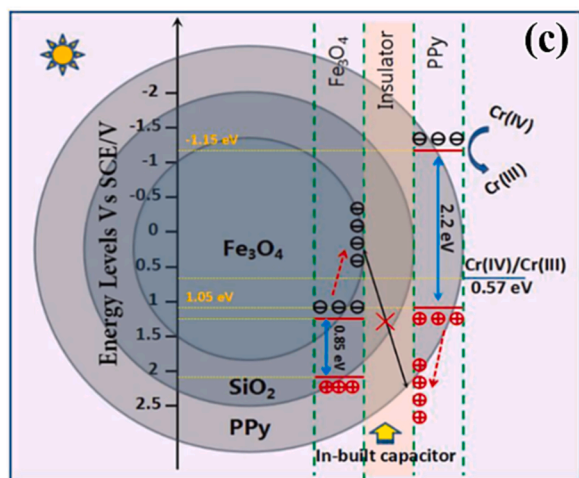
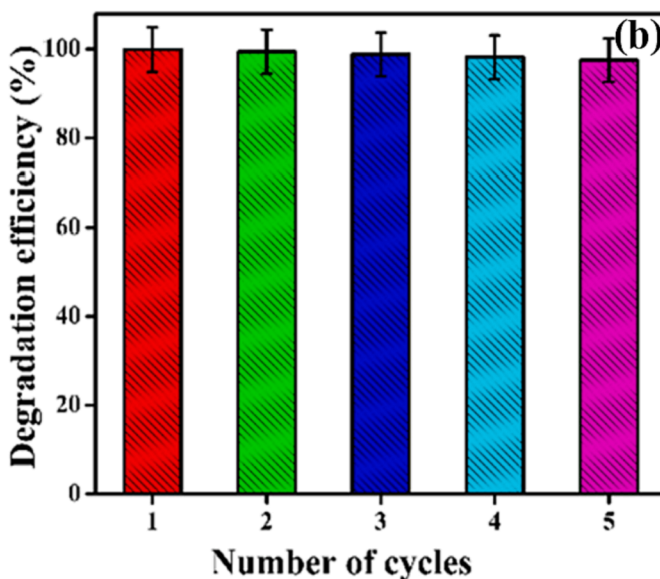
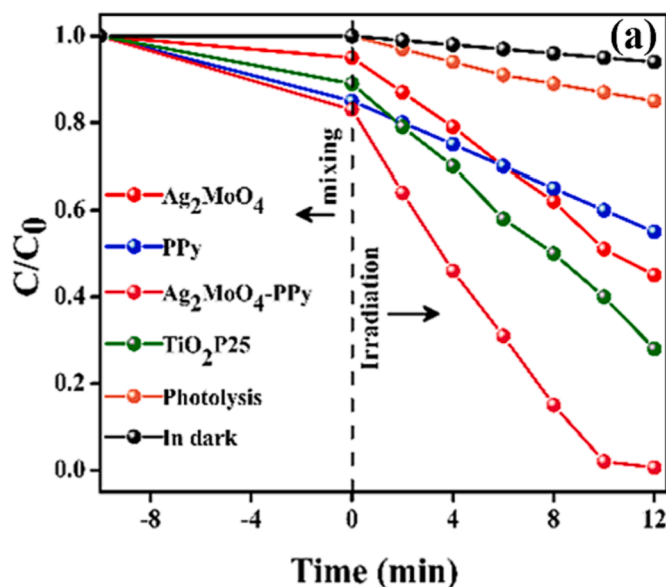


Fig. 11. (a) Comparison chart for degradation efficiency by different catalysts; (b) Recycling efficiency of $\text{Ag}_2\text{MoO}_4/\text{PPy}$ photocatalyst during Cr(VI) reduction process.

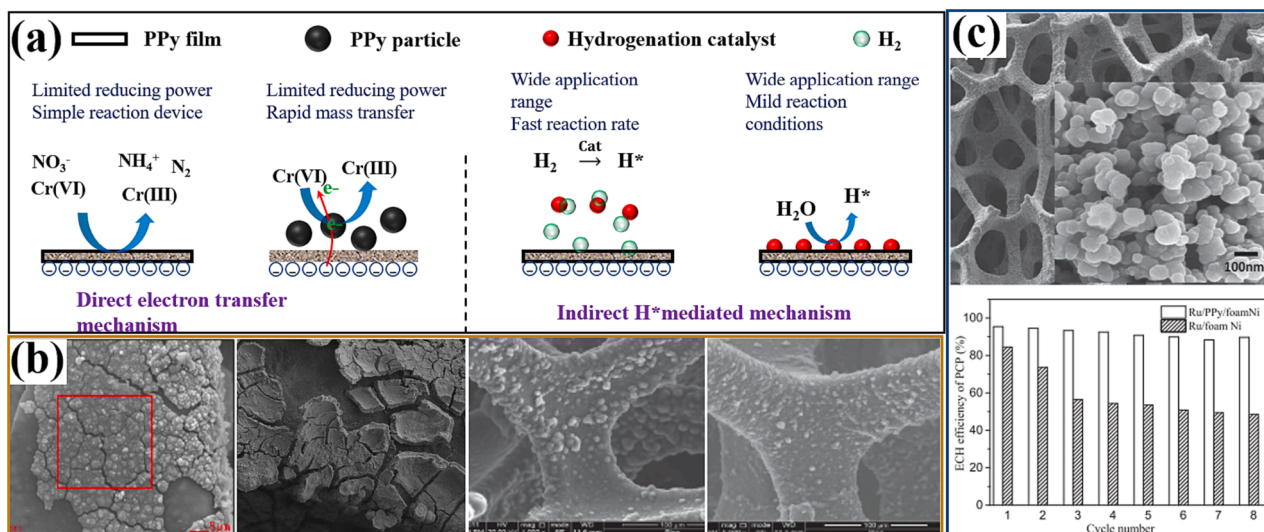


Fig. 12. (a) Application strategy of PPy in electroreduction water treatment technology; (b) Morphology of PPy deposited on foam nickel electrode [Reprinted with permission from Ref. [116,117]. Copyright, Elsevier and American Chemical Society]; Electroreduction dechlorination efficiency of PCP with cycle number on the Ru/PPy/foam Ni and Ru/foam Ni electrode [Reprinted with permission from Ref. [118]. Copyright 2019, Elsevier].

reduction by $\text{Fe}_3\text{O}_4/\text{SiO}_2/\text{PPy}$ ternary heterostructures; (d) Photocurrents of PPy and $\text{Fe}_3\text{O}_4/\text{SiO}_2/\text{PPy}$ heterostructures without bias under model sunlight [Reprinted with permission from Ref. [113]. Copyright 2020, Elsevier].

Electroreduction: PPy can achieve Cr(VI) reduction through direct electron transfer. It should be noted that PPy as cathode will repel Cr(VI) due to the electronegativity of the electrode surface, which is not conducive to adsorption and reduction processes. In response to this issue, enhanced mass transfer operations have been carried out by constructing flow-through electrodes and particle electrodes, which can effectively enhance Cr(VI) reduction [114]. PPy can also serve as a mediator material to assist in the hydrogenation reduction of pollutants in water. Chen et al. used PPy/Ti as the cathode and Pd/Cu bimetallic catalyst to achieve selective reduction of NO_3^- in water. Among them, the PPy/Ti cathode exhibited excellent hydrogenation reduction ability and repelled the direct reduction of NO_3^- to NH_4^+ on the cathode. After 90 min, the NO_3^- removal rate reached 100%, and the N_2 selectivity reached 93%~95% [115].

Currently, the noble metal-PPy-foam nickel electrode has attracted much attention. As the conductive intermediate layer of the noble metal modified electrode, PPy can effectively reduce the amount of noble metal and contact resistance. Meanwhile, the participation of noble metals achieved efficient hydrogenation reduction using atomic hydrogen (H^*) as the active species, which can achieve hydrogenation reduction of high valent oxygen radicals and reduction dehalogenation [116–118]. Furthermore, composite modifications can be carried out on noble metals and PPy, such as the electrode of Pd-Ni/PPy-rGO/Ni. Compared with a single PPy intermediate layer and Pd modified electrode, this modified electrode had lower impedance and higher hydrogenation performance [119]. Application strategy of PPy in electroreduction water treatment technology is shown in Fig. 12a.

For the problem of PPy film shedding, foam Ni was used as electrode substrate, the research showed that PPy film materials with different morphology and load strength can be obtained by adjusting the electrodeposition parameters (Fig. 12b). Among them, potential, electrolyte and deposition time were the main influencing factors [116]. Wang et al. prepared Ru/PPy/foam Ni active cathode by adjusting deposition parameters, and showed good reuse performance for PCP (pentachlorophenol) (Fig. 12c) [118]. Unfortunately, the balance between PPy membrane microstructure and interfacial strength had received little attention.

Catalytic hydrogenation: During the electro reduction process,

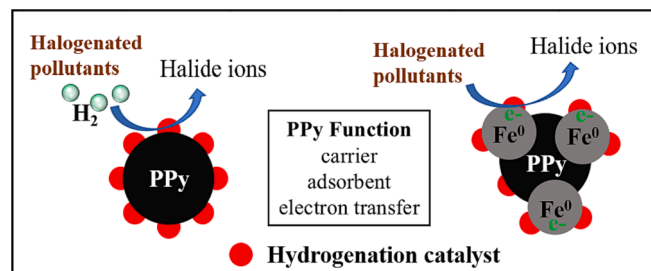


Fig. 13. Catalytic hydrogenation technology and its mechanism involved by PPy.

PPy-based cathode will hinder the adsorption process of negatively charged pollutants, which is not conducive to their hydrogenation reduction. By directly loading the hydrogenation catalyst onto PPy or its composite materials and introducing an external reducing agent (H_2), a good catalytic hydrogenation system can be constructed to achieve the coadsorption reduction process of pollutants [120]. To overcome the problem of catalyst recovery, PPy can be used to coat ferromagnetic materials to achieve catalyst magnetic recovery performance [121].

In addition, PPy can also be combined with Fe^0 reduction technology. Lei et al. designed Pd/Fe@PPY catalysts, the introduction of PPy can avoid nZVI oxidation deactivation and agglomeration, while promoting electron transfer and pollutant adsorption processes. Compared with exposed Pd/Fe nanoparticles, Pd/Fe@PPY increased reactivity to 4-CP by nearly 8-fold [122]. The application of PPy in catalytic hydrogenation systems is shown in Fig. 13.

3.3. Antibacterial and disinfection technology

Due to the strong electrostatic interaction between the positive charge on the PPy chain and the bacterial cell wall, the PPy coating material with polycationic skeleton can destroy the microbial cell membrane by stopping cellular respiration, and has good inhibitory effect on both gram-positive and gram-negative bacteria [123]. In addition, PPy can achieve enhanced antibacterial activity by combining with other types of antibacterial materials, such as metal based nanomaterials, natural materials etc. [124,125]. Compared with conventional water disinfection methods such as chlorine disinfection, ozone

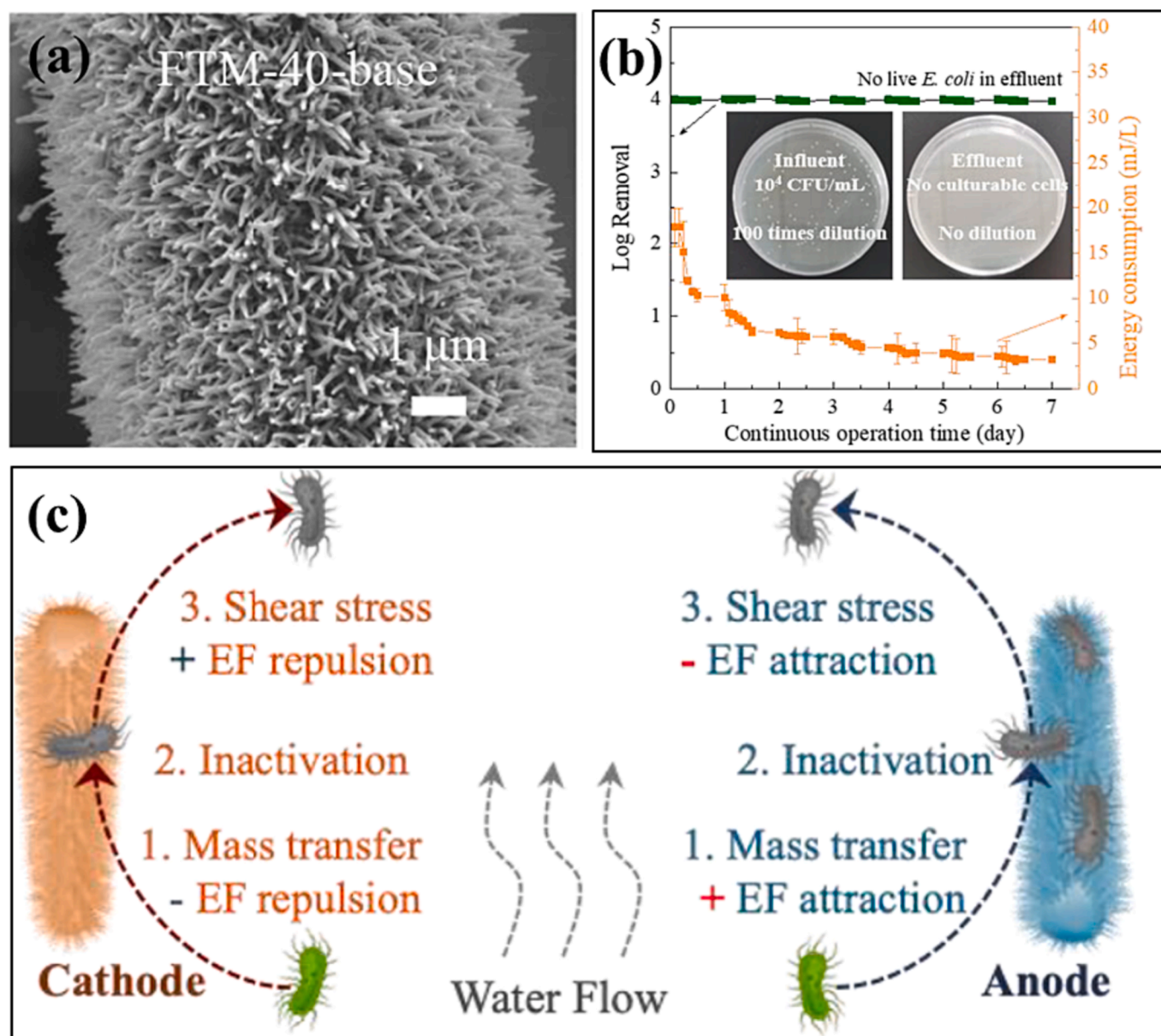


Fig. 14. (a) SEM images of the PPyNWs on the carbon fiber (b) The durability performance and energy consumption of the FTM-40 EDD operated using *E. coli*-contaminated tap water at 1.0 V and 2000 L/m²/h. (c) Mechanism diagram of electroporation disinfection technology of PPy applied to cathode and anode [Reprinted with permission from Ref. [129]. Copyright 2021, Elsevier].

disinfection, and ultraviolet disinfection, the use of PPy-based antibacterial disinfection materials has the advantages of green, energy-saving, and no secondary pollution.

Fernando A.G. da Silva Jr et al. studied the antibacterial performance of branched PPy, conventional PPy, highly soluble PPy, and PPy-Ag colloids against *Escherichia coli*, *Staphylococcus aureus*, and *Klebsiella pneumoniae* in terms of factors affecting the antibacterial performance of PPy based materials. The experimental data showed that different forms of PPy had different antibacterial abilities, and different strains had different response strengths to different PPy based antibacterial materials. Based on this, it is proposed that the antibacterial behavior of PPy based materials depends on various structural parameters, such as surface area, aggregation level, and additives [126].

Based on the engineering application of PPy based antibacterial materials, some composite technologies for water pollution control have been developed. Sun et al. prepared PPy modified PVDF antibacterial films and developed membrane technologies for biological pollution

resistance through synergistic electric repulsion [127]; Liao et al. incorporated PPy nanospheres into the polyamide layer to obtain a chlorine resistant antibacterial membrane, which simultaneously increased the membrane's service life and water flux [128]; Xu et al. deposited Ag nanoparticles on PPy coated fabrics to obtain an antibacterial photothermal film [90].

The electroporation disinfection and sterilization technology is a newly developed drinking water disinfection technology in recent years, which has the advantages of low energy consumption, good effect and no secondary pollution. Its most common method is to prepare nanowire modified electrodes, and use the space scale effect of nanowires to generate a strong electric field near the tip of nanowires to kill bacteria by electroporation under low external voltage. Pi et al. prepared PPy nanowires on three-dimensional graphite felt fibers through a flow-through reactor, and conducted disinfection experiments at a voltage of 1.0 V and a flow rate of 2000 L/m²/h (Fig. 14a). The disinfection device can remove more than 4-log *Escherichia coli* from tap water within

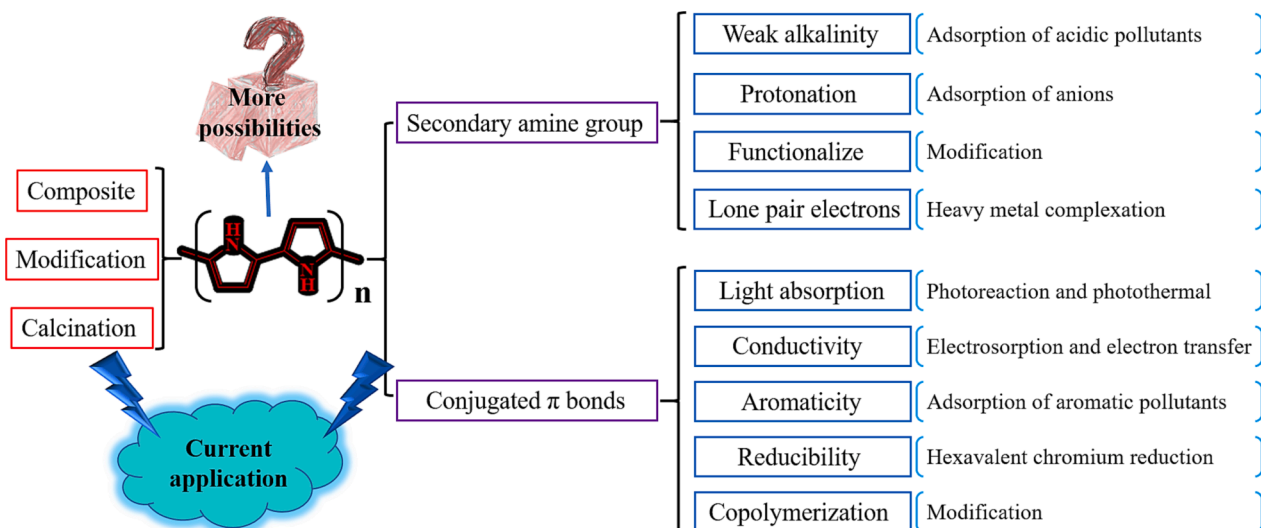


Fig. 15. The relationship between the physicochemical properties, design scheme, and application fields of PPy.

7 days of operation, and the energy consumption was <20 mJ/L (Fig. 14b). It was found that in the process of cathode disinfection, the convective mass transfer in the porous PPyNWs cathode overcame the electric field repulsion between the negative charged *Escherichia coli* cells, promoted the cells to be exposed to the strong electric field near PPyNWs, and contributed to the inactivation of *Escherichia coli*. However, due to the electric attraction between anode and negatively charged *Escherichia coli* cells, its electroporation inactivation of *Escherichia coli* was greater than that of cathode (Fig. 14c) [129].

3.4. Other applications

Nitrided carbon materials have excellent physicochemical properties and are a promising environmental functional material. PPy is a good precursor for obtaining pyrrole nitrogen.

Shi et al. prepared PPy nanotubes through template method, and then calcined them in N_2 atmosphere at $900^\circ C$ to obtain nitrogen doped carbon nanotubes. It is found that carbonization increased the specific surface area of the nanotubes from $19.5\text{ m}^2/\text{g}$ to $200.9\text{ m}^2/\text{g}$, and significantly enhanced their conductivity, wettability, and sodium ion absorption efficiency [130]. Wang et al. prepared a composite photocatalyst (FeP/CoP-N-C) by calcining PPy. Characterization showed that the d-band center of FeP/CoP-N-C-700 with carbon/oxygen double defects was -1.35 eV , which demonstrated excellent n-type conductivity and charge separation efficiency, enabling rapid photocatalytic degradation of levofloxacin [131]. Hu et al. used the carbonization product of PPy at $800^\circ C$ for the activation of PMS to degrade phenol in water. Experimental data showed that this catalyst can activate PMS through a none free radical pathway over a wide pH range (2–9) [132].

4. Thought and outlook

PPy plays a crucial role in the field of water pollution control, owing to its comprehensive physicochemical properties, such as morphology plasticity, template encapsulation ability, ion exchange ability, light absorption ability, electron transport ability, antibacterial ability, among others. Based on existing research, the correlation between the application of PPy and its physicochemical properties is shown in Fig. 15. From the perspective of molecular structure, the secondary amine group and conjugation π bonds are the source of its widespread application. Moreover, specific PPy-based nanomaterials can be obtained through coupling, modification, and calcination methods, which is beneficial for expanding the application range of PPy and enhancing its related properties. However, there are several challenges that need to

be addressed.

- (1) The molecular structure of PPy in oxidation state and reduction state is not yet clear. Based on the principle of oxidation–reduction reaction, the possible molecular structures of PPy in oxidation and reduction states are given in this work (Section 3.1.1). However, in order to meet the future demand for more refined material development, it is necessary to conduct sufficient research on the molecular configurations and physicochemical properties of PPy in different chemical states.
- (2) Neglecting the impact of PPy polymerization degree on light absorption and electric conductivity, the issues of light absorption and conductivity with different polymerization degrees, the existence of group effects, and the ability to finely regulate their polymerization degree are all worth studying and considering. This is of great significance for water pollution control technologies involving photon and electron transfer.
- (3) For PPy based composite materials, excessive attention is paid to the coupling promotion effect, and there are few reports on the impact of PPy structure design and preparation parameters on combined material performance. Meanwhile, the research on highly ordered PPy nanomaterials is insufficient, which limits their potential for application in more fields.

In addition, the application research field of PPy should be narrowed down to achieve key breakthroughs. The future research directions of PPy should focus on adsorption of negatively charged pollutants, membrane separation technology, photothermal technology, photooxidation technology, electroreduction technology, and antibacterial technology. In summary, the specific research work of PPy includes: 1) Comprehensively establish the relationship between preparation parameters, structure, and physicochemical properties; 2) Prepare highly ordered PPy nanomaterials and study their application potential; 3) Develop more PPy grafting modification strategies to obtain more high-performance PPy based functional materials; 4) Actively explore the possibility of technology joint application and fully utilize the multi-functional advantages of PPy.

Declaration of Competing Interest

The authors declare that they have no known competing financial interests or personal relationships that could have appeared to influence the work reported in this paper.

Data availability

No data was used for the research described in the article.

Acknowledgments

This study was financially supported by the National Natural Science Foundation of China (42122057, 41977308), the Central Plain Talent Program of Henan Province (ZYYCYU202012168), the Henan Post-doctoral Science Foundation (HN2022030), the Scientific Research Starting Foundation of Henan Normal University (5101219470261, 5101219170856).

References

- [1] Y. Wu, S. Wang, Z. Ni, H. Li, L. May, J. Pu, Emerging water pollution in the world's least disturbed lakes on Qinghai-Tibetan Plateau, *Environ. Pollut.* 272 (2021), 116032.
- [2] Y. Liu, P. Wang, B. Gojenko, J. Yu, L. Wei, D. Luo, T. Xiao, A review of water pollution arising from agriculture and mining activities in Central Asia: Facts, causes and effects, *Environ. Pollut.* 291 (2021), 118209.
- [3] M. Kah, G. Sigmund, F. Xiao, T. Hofmann, Sorption of ionizable and ionic organic compounds to biochar, activated carbon and other carbonaceous materials, *Water Res.* 124 (2017) 673–692.
- [4] X. Liu, W. Wei, J. Xu, L.S. Dongbo Wang d, B.J. Ni, Photochemical decomposition of perfluorochemicals in contaminated water, *Water Res.* 186 (2020), 116311.
- [5] Z. Cai, X. Hu, Z. Li, H. He, T. Li, H. Yuan, Y. Zhang, B. Tan, J. Wang, Hypercrosslinking porous polymer layers on TiO₂-graphene photocatalyst: enhanced adsorption of water pollutants for efficient degradation, *Water Res.* 227 (2022), 119341.
- [6] B.C.K. Tee, J. Ouyang, Soft electronically functional polymeric composite materials for a flexible and stretchable digital future, *Adv. Mater.* 30 (2018) 1802560.
- [7] H. Zhou, J. Peng, X. Duan, H. Yin, B. Huang, C. Zhou, S. Zhong, H. Zhang, P. Zhou, Z. Xiong, Z. Ao, S. Wang, G. Yao, B. Lai, Redox-active polymers as robust electron-shuttle co-catalysts for fast Fe³⁺/Fe²⁺ circulation and green fenton oxidation, *Environ. Sci. Tech.* 57 (2023) 3334–3344.
- [8] T. Wang, L. Yan, Y. He, S.I. Alhassan, H. Gang, B. Wu, L. Jin, H. Wang, Application of polypyrrole-based adsorbents in the removal of fluoride: a review, *RSC Adv.* 12 (2022) 3505–3517.
- [9] R. Kumar, P. Raizada, T. Ahamad, S.M. Alshehri, Q.V. Le, T.S. Alomar, V. H. Nguyen, R. Selvasembian, S. Thakur, D.C. Nguyen, P. Singh, Polypyrrole-based nanomaterials: A novel strategy for reducing toxic chemicals and others related to environmental sustainability applications, *Chemosphere* 303 (2022), 134993.
- [10] S.M. Abu-Sari, M.F.A. Patah, B.C. Ang, W.M.A.W. Daud, A review of polymerization fundamentals, modification method, and challenges of using PPy-based photocatalyst on perspective application, *J. Environ. Chem. Eng.* 10 (2022), 108725.
- [11] F.A.G.d. Silva Júnior, S.A. Vieira, S.d.A. Botton, M.M.d. Costa, H.P.d. Oliveira, Antibacterial activity of polypyrrole-based nanocomposites: a mini-review, *Polímeros* 30 (2020) 2020048.
- [12] X. Yuan, D. Floresyona, P.-H. Aubert, T.T. Bui, S. Remita, S. Ghosh, F. Brisset, F. Goubard, H. Remita, Photocatalytic degradation of organic pollutant with polypyrrole nanostructures under UV and visible light, *Appl. Catal. B: Environ.* 242 (2019) 284–292.
- [13] H. Yu, Y. He, G. Xiao, H. Li, X. Mei, Y. Cheng, F. Zhong, L. Zhou, J.Z. Ou, Intercalation of soft PPy polymeric nanoparticles in graphene oxide membrane for enhancing nanofiltration performances, *Sep. Purif. Technol.* 272 (2021), 118933.
- [14] S. Balser, J. Bernd, L. Fritsche, A. Terfort, Preparation and characterization of highly conductive and biorepulsive polypyrrole/polyglycerol surface films, *ACS Appl. Polym. Mater.* 4 (2022) 8344–8356.
- [15] Y. Wang, C. Liang, C. Fan, J. Chen, Z. Zhang, H. Liu, Composite modification of carbon fiber cathode with tree-like branched polypyrrole-microwires and polyaniline-nanorods for enhancing hexavalent chromium reduction, *Environ. Sci. Nano* 10 (2023) 891–901.
- [16] H. Kang, D. Zhang, X. Chen, H. Zhao, D. Yang, Y. Li, M. Bao, Z. Wang, Preparation of MOF/polypyrrole and flower-like MnO₂ electrodes by electrodeposition: High-performance materials for hybrid capacitive deionization defluorination, *Water Res.* 229 (2023), 119441.
- [17] Y. Zhao, C. Zhao, Y. Yang, Z. Li, X. Qiu, J. Gao, M. Ji, Adsorption of sulfamethoxazole on polypyrrole decorated volcanics over a wide pH range: mechanisms and site energy distribution consideration, *Sep. Purif. Technol.* 283 (2022), 120165.
- [18] M. Wu, S. Ding, L. Deng, X. Wang, PPY nanotubes-enabled in-situ heating nanofibrous composite membrane for solar-driven membrane distillation, *Sep. Purif. Technol.* 281 (2022), 119995.
- [19] J. Ren, C. Wang, J. Ding, T. Li, Y. Ma, Magnetic Core-Shell Fe₃O₄@polypyrrole@4-vinylpyridine composites for the removal of multiple dyes, *ACS Appl. Polym. Mater.* 4 (2022) 9449–9462.
- [20] Y. Li, Y. Gao, Q. Zhang, R. Wang, C. Li, J. Mao, L. Guo, F. Wang, Z. Zhang, L. Wang, Flexible and free-standing pristine polypyrrole membranes with a nanotube structure for repeatable Cr(VI) ion removal, *Sep. Purif. Technol.* 258 (2021), 117981.
- [21] A.L. Pang, A. Arsad, M. Ahmadipour, Synthesis and factor affecting on the conductivity of polypyrrole: a short review, *Polym. Adv. Technol.* 32 (2020) 1428–1454.
- [22] J. John, S. Jayalekshmi, Polypyrrole with appreciable solubility, crystalline order and electrical conductivity synthesized using various dopants appropriate for device applications, *Polym. Bull.* 80 (2022) 6099–6116.
- [23] J. Stejskal, I. Sapurina, J. Vilčáková, M. Jurča, M. Trchová, Z. Kolská, J. Prokeš, I. Krivka, One-pot preparation of conducting melamine/polypyrrole/magnetite ferrosponge, *ACS Appl. Polym. Mater.* 3 (2021) 1107–1115.
- [24] M. Tanzifi, M. Tavakkoli Yarak, Z. Beiranzadeh, L. Heidarpour Saremi, M. Najafifard, H. Moradi, M. Mansouri, M. Karami, H. Bazgir, Carboxymethyl cellulose improved adsorption capacity of polypyrrole/CMC composite nanoparticles for removal of reactive dyes: experimental optimization and DFT calculation, *Chemosphere* 255 (2020), 127052.
- [25] D. Ma, Y. Wang, X. Han, S. Xu, J. Wang, Applicable tolerance evaluations of ion-doped carbon nanotube/polypyrrole electrode under adverse solution conditions for capacitive deionization process, *Sep. Purif. Technol.* 201 (2018) 167–178.
- [26] X. Ma, X. Jia, H. Gao, D. Wen, Polypyrrole-dopamine nanofiber light-trapping coating for efficient solar vapor generation, *ACS Appl. Mater. Interfaces* 13 (2021) 57153–57162.
- [27] W. Zhang, Y. Zhou, K. Feng, J. Trinidad, A. Yu, B. Zhao, Morphologically controlled bioinspired dopamine-polypyrrole nanostructures with tunable electrical properties, *Adv. Electron. Mater.* 1 (2015) 1500205.
- [28] W. Zhang, Z. Pan, F.K. Yang, B. Zhao, A Facile In situ approach to polypyrrole functionalization through bioinspired catechols, *Adv. Funct. Mater.* 25 (2015) 1588–1597.
- [29] M. Khosravi, S. Azizian, Preparation of superhydrophobic and superoleophilic nanostructured layer on steel mesh for oil-water separation, *Sep. Purif. Technol.* 172 (2017) 366–373.
- [30] M. Zheng, Y. Wei, J. Ren, B. Dai, W. Luo, M. Ma, T. Li, Y. Ma, 2-aminopyridine functionalized magnetic core-shell Fe₃O₄@polypyrrole composite for removal of Mn (VII) from aqueous solution by double-layer adsorption, *Sep. Purif. Technol.* 277 (2021), 119455.
- [31] R.S. Aliabadi, N.O. Mahmoodi, Synthesis and characterization of polypyrrole, polyaniline nanoparticles and their nanocomposite for removal of azo dyes; sunset yellow and Congo red, *J. Clean. Prod.* 179 (2018) 235–245.
- [32] X.Y. Shi, M.H. Gao, W.W. Hu, D. Luo, S.Z. Hu, T. Huang, N. Zhang, Y. Wang, Largely enhanced adsorption performance and stability of MXene through in-situ depositing polypyrrole nanoparticles, *Sep. Purif. Technol.* 287 (2022), 120596.
- [33] J.B. Feng, Y.Y. Li, Y. Zhang, Y.Y. Xu, X.W. Cheng, Adsorptive removal of indomethacin and diclofenac from water by polypyrrole doped-GO/COF-300 nanocomposites, *Chem. Eng. J.* 429 (2022), 132499.
- [34] C. Huyan, S. Ding, Z. Lyu, M.H. Engelhard, Y. Tian, D. Du, D. Liu, Y. Lin, Selective removal of perfluorobutyric acid using an electroactive ion exchanger based on polypyrrole@iron oxide on carbon cloth, *ACS Appl. Mater. Interfaces* 13 (2021) 48500–48507.
- [35] W. Yuan, S.I. Etkind, S.L. Luo, H. Feng, D. Fong, T.M. Swager, Cyclodextrin-functionalized polypyrrole particles for the extraction of aromatics from water, *ACS Appl. Mater. Interfaces* 14 (2022) 45904–45909.
- [36] F. Huang, X. Tian, W. Wei, X. Xu, J. Li, Y. Guo, Z. Zhou, Wheat straw-core hydrogel spheres with polypyrrole nanotubes for the removal of organic dyes, *J. Clean. Prod.* 344 (2022), 131100.
- [37] M. Chen, Z. Yan, J. Luan, X. Sun, W. Liu, X. Ke, π - π electron-donor-acceptor (EDA) interaction enhancing adsorption of tetracycline on 3D PPY/CMC aerogels, *Chem. Eng. J.* 454 (2023), 140300.
- [38] Y. Tian, J. Xing, C. Huyan, C. Zhu, D. Du, W. Zhu, Y. Lin, I. Chowdhury, Electrically controlled anion exchange based on a polypyrrole/carbon cloth composite for the removal of perfluorooctanoic acid, *ACS ES&T Water* 1 (2021) 2504–2512.
- [39] S. Hong, F.S. Cannon, P. Hou, T. Byrne, C. Nieto-Delgado, Adsorptive removal of sulfate from acid mine drainage by polypyrrole modified activated carbons: effects of polypyrrole deposition protocols and activated carbon source, *Chemosphere* 184 (2017) 429–437.
- [40] A. Mullick, S. Neogi, Ultrasound assisted synthesis of Mg-Mn-Zr impregnated activated carbon for effective fluoride adsorption from water, *Ultrason. Sonochem.* 50 (2019) 126–137.
- [41] Y.J. Ko, K. Choi, S. Lee, K.W. Jung, S. Hong, H. Mizuseki, J.W. Choi, W.S. Lee, Strong chromate-adsorbent based on pyrrolic nitrogen structure: an experimental and theoretical study on the adsorption mechanism, *Water Res.* 145 (2018) 287–296.
- [42] L. Xiang, C.G. Niu, N. Tang, X.X. Lv, H. Guo, Z.W. Li, H.Y. Liu, L.S. Lin, Y.Y. Yang, C. Liang, Polypyrrole coated molybdenum disulfide composites as adsorbent for enhanced removal of Cr(VI) in aqueous solutions by adsorption combined with reduction, *Chem. Eng. J.* 408 (2021), 127281.
- [43] Z.A. Chaleshtari, R. Foudazi, Polypyrrole@polyHIPE composites for hexavalent chromium removal from water, *ACS Appl. Polym. Mater.* 2 (2020) 3196–3204.
- [44] J. Wang, C. Luo, G. Qi, K. Pan, B. Cao, Mechanism study of selective heavy metal ion removal with polypyrrole-functionalized polyacrylonitrile nanofiber mats, *Appl. Surf. Sci.* 316 (2014) 245–250.
- [45] S. Zhang, Y. Shao, J. Liu, I.A. Aksay, Y. Lin, Graphene-polypyrrole nanocomposite as a highly efficient and low cost electrically switched ion exchanger for removing ClO₄ from wastewater, *ACS Appl. Mater. Interfaces* 3 (2011) 3633–3637.
- [46] R. Karthik, S. Meenakshi, Chemical modification of chitin with polypyrrole for the uptake of Pb(II) and Cd(II) ions, *Int. J. Biol. Macromol.* 78 (2015) 157–164.

- [47] F. Zhou, Y. Li, S. Wang, X. Wu, J. Peng, F. Wang, L. Wang, J. Mao, Turning waste into valuables: In situ deposition of polypyrrole on the obsolete mask for Cr(VI) removal and desalination, *Sep. Purif. Technol.* 306 (2023), 122643.
- [48] U.O. Aigbe, R. Das, W.H. Ho, V. Srinivasu, A. Maity, A novel method for removal of Cr(VI) using polypyrrole magnetic nanocomposite in the presence of unsteady magnetic fields, *Sep. Purif. Technol.* 194 (2018) 377–387.
- [49] H. Wang, X. Yuan, Y. Wu, X. Chen, L. Leng, H. Wang, H. Li, G. Zeng, Facile synthesis of polypyrrole decorated reduced graphene oxide-Fe₃O₄ magnetic composites and its application for the Cr(VI) removal, *Chem. Eng. J.* 262 (2015) 597–606.
- [50] Y. Xu, J. Chen, R. Chen, P. Yu, S. Guo, X. Wang, Adsorption and reduction of chromium(VI) from aqueous solution using polypyrrole/calcium rectorite composite adsorbent, *Water Res.* 160 (2019) 148–157.
- [51] J. Wang, K. Pan, Q. He, B. Cao, Polyacrylonitrile/polypyrrole core/shell nanofiber mat for the removal of hexavalent chromium from aqueous solution, *J. Hazard. Mater.* 244–245 (2013) 121–129.
- [52] F.L. Long, C.G. Niu, N. Tang, H. Guo, Z.W. Li, Y.Y. Yang, L.S. Lin, Highly efficient removal of hexavalent chromium from aqueous solution by calcined Mg/Al-layered double hydroxides/polyaniline composites, *Chem. Eng. J.* 404 (2021), 127084.
- [53] L. Zhou, T. Chi, Y. Zhou, J. Lv, H. Chen, S. Sun, X. Zhu, H. Wu, X. Hu, Efficient removal of hexavalent chromium through adsorption-reduction-adsorption pathway by iron-clay biochar composite prepared from *Populus nigra*, *Sep. Purif. Technol.* 285 (2022), 120386.
- [54] R. Yan, X. Feng, L. Kong, Q. Wan, W. Zheng, T. Hagio, R. Ichino, X. Cao, L. Li, Evenly distribution of amorphous iron sulfides on reconstructed Mg-Al hydroxalicates for improving Cr(VI) removal efficiency, *Chem. Eng. J.* 417 (2021), 129228.
- [55] Y. Sun, F. Yu, L. Li, J. Ma, Adsorption-reduction synergistic effect for rapid removal of Cr (VI) ions on superelastic NH₂-graphene sponge, *Chem. Eng. J.* 421 (2021), 129933.
- [56] T. Lü, R. Ma, K. Ke, D. Zhang, D. Qi, H. Zhao, Synthesis of gallic acid functionalized magnetic hydrogel beads for enhanced synergistic reduction and adsorption of aqueous chromium, *Chem. Eng. J.* 408 (2021), 127327.
- [57] J. Song, Z. Meng, X. Wang, G. Zhang, C. Bi, J. Hou, One-step microwave method synthesis of Fe₃O₄ nanoribbon@carbon composite for Cr (VI) removal, *Sep. Purif. Technol.* 298 (2022), 121530.
- [58] K. Gao, J. Li, M. Chen, Y. Jin, Y. Ma, G. Ou, Z. Wei, ZIF-67 derived magnetic nanoporous carbon coated by po(m-phenylenediamine) for hexavalent chromium removal, *Sep. Purif. Technol.* 277 (2021), 119436.
- [59] M. Bhaumik, T.Y. Leswif, A. Maity, V.V. Srinivasu, M.S. Onyango, Removal of fluoride from aqueous solution by polypyrrole/Fe₃O₄ magnetic nanocomposite, *J. Hazard. Mater.* 186 (2011) 150–159.
- [60] J. Chen, C. Shu, N. Wang, J. Feng, H. Ma, W. Yan, Adsorbent synthesis of polypyrrole/TiO₂ for effective fluoride removal from aqueous solution for drinking water purification: adsorbent characterization and adsorption mechanism, *J. Colloid Interface Sci.* 495 (2017) 44–52.
- [61] Z. Wang, S. Tian, J. Niu, W. Kong, J. Lin, X. Hao, G. Guan, An electrochemically switched ion exchange process with self-electrical-energy recuperation for desalination, *Sep. Purif. Technol.* 239 (2020), 116521.
- [62] L. Miao, Z. Wang, J. Peng, W. Deng, W. Chen, Q. Dai, T. Ueyama, Pseudocapacitive deionization with polypyrrole grafted CMC carbon aerogel electrodes, *Sep. Purif. Technol.* 296 (2022), 121441.
- [63] D. Ma, Y. Wang, X. Han, S. Xu, J. Wang, Electrode configuration optimization of capacitive deionization cells based on zero charge potential of the electrodes, *Sep. Purif. Technol.* 189 (2017) 467–474.
- [64] G. Tan, S. Lu, N. Xu, D. Gao, X. Zhu, Pseudocapacitive behaviors of polypyrrole grafted activated carbon and MnO₂ electrodes to enable fast and efficient membrane-free capacitive deionization, *Environ. Sci. Tech.* 54 (2020) 5843–5852.
- [65] Y. Zhao, Y. Cai, Y. Wang, S. Xu, A win-win strategy of β -cyclodextrin and ion-doped polypyrrole composite nanomaterials for asymmetric capacitive deionization, *Sep. Purif. Technol.* 259 (2021), 118175.
- [66] J. Shen, S. Zhang, Z. Zeng, J. Huang, Y. Shen, Y. Guo, Synthesis of magnetic short-channel mesoporous silica SBA-15 modified with a polypyrrole/polyaniline copolymer for the removal of mercury ions from aqueous solution, *ACS Omega* 6 (2021) 25791–25806.
- [67] M. Ghorbani, H. Eisazadeh, Removal of COD, color, anions and heavy metals from cotton textile wastewater by using polyaniline and polypyrrole nanocomposites coated on rice husk ash, *Compos. B Eng.* 45 (2013) 1–7.
- [68] Z. Guo, M. Shams, C. Zhu, Q. Shi, Y. Tian, M.H. Engelhard, D. Du, I. Chowdhury, Y. Lin, Electrically switched ion exchange based on carbon-polypyrrole composite smart materials for the removal of ReO₄ from aqueous solutions, *Environ. Sci. Tech.* 53 (2019) 2612–2617.
- [69] J. Luo, X. Du, F. Gao, H. Kong, X. Hao, A. Abudula, G. Guan, X. Ma, B. Tang, An electrochemically switchable triiodide-ion-imprinted PPy membrane for highly selective recognition and continuous extraction of iodide, *Sep. Purif. Technol.* 251 (2020), 117312.
- [70] H. Yu, L. Zhou, Z. Li, Y. Liu, X. Ao, J. Ouyang, Z. Le, Z. Liu, A.A. Adesina, Electrodeposited polypyrrole/biomass-derived carbon composite electrodes with high hybrid capacitance and hierarchical porous structure for enhancing U(VI) electrosorption from aqueous solution, *Sep. Purif. Technol.* 302 (2022), 122169.
- [71] X. Tan, C. Hu, Z. Zhu, H. Liu, J. Qu, Electrically pore-size-tunable polypyrrole membrane for antifouling and selective separation, *Adv. Funct. Mater.* 29 (2019) 1903081.
- [72] L. Shao, X. Cheng, Z. Wang, J. Ma, Z. Guo, Tuning the performance of polypyrrole-based solvent-resistant composite nanofiltration membranes by optimizing polymerization conditions and incorporating graphene oxide, *J. Membrane Sci.* 452 (2014) 82–89.
- [73] M.R. Mahdavi, M. Delnavaz, V. Vatanpour, J. Farahbakhsh, Effect of blending polypyrrole coated multiwalled carbon nanotube on desalination performance and antifouling property of thin film nanocomposite nanofiltration membranes, *Sep. Purif. Technol.* 184 (2017) 119–127.
- [74] Q. Xu, Y. Liu, Y. Wang, Y. Song, C. Zhao, L. Han, Synergistic oxidation-filtration process of electroactive peroxydisulfate with a cathodic composite CNT-PPy/PVDF ultrafiltration membrane, *Water Res.* 210 (2022), 117971.
- [75] R.A. Tufa, T. Piallat, J. Hnat, E. Fontananova, M. Paidar, D. Chanda, E. Curcio, G. di Profio, K. Bouzek, Salinity gradient power reverse electrodialysis: Cation exchange membrane design based on polypyrrole-chitosan composites for enhanced monovalent selectivity, *Chem. Eng. J.* 380 (2020), 122461.
- [76] Y. Zhou, C. Hu, H. Liu, J. Qu, Potassium-ion recovery with a polypyrrole membrane electrode in novel redox transistor electrodialysis, *Environ. Sci. Tech.* 54 (2020) 4592–4600.
- [77] X. Pang, X. Yu, Y. He, S. Dong, X. Zhao, J. Pan, R. Zhang, L. Liu, Preparation of monovalent cation perm-selective membranes by controlling surface hydration energy barrier, *Sep. Purif. Technol.* 270 (2021), 118768.
- [78] Y. Dong, Y. Tan, K. Wang, Y. Cai, J. Li, C. Sonne, C. Li, Reviewing wood-based solar-driven interfacial evaporators for desalination, *Water Res.* 223 (2022), 119011.
- [79] Y. Xu, J. Wang, F. Yu, Z. Guo, H. Cheng, J. Yin, L. Yan, X. Wang, Flexible and efficient solar thermal generators based on polypyrrole coated natural latex foam for multimedia purification, *ACS Sustain. Chem. Eng.* 8 (2020) 12053–12062.
- [80] Y.C. Wang, C.Z. Wang, X.J. Song, M.H. Huang, S.K. Megarajan, S.F. Shaikat, H. Q. Jiang, Improved light-harvesting and thermal management for efficient solar-driven water evaporation using 3D photothermal cones, *J. Mater. Chem. A* 6 (2018) 9874–9881.
- [81] Y. Pan, E. Li, Y. Wang, C. Liu, C. Shen, X. Liu, Simple design of a porous solar evaporator for salt-free desalination and rapid evaporation, *Environ. Sci. Tech.* 56 (2022) 11818–11826.
- [82] Y. Wang, X. Sun, S. Tao, Rational 3D coiled morphology for efficient solar-driven desalination, *Environ. Sci. Tech.* 54 (2020) 16240–16248.
- [83] Z. Xie, J. Zhu, L. Zhang, Three-dimensionally structured polypyrrole-coated setaria viridis spike composites for efficient solar steam generation, *ACS Appl. Mater. Interfaces* 13 (2021) 9027–9035.
- [84] Y. Xu, T. Xu, Y. Guo, W. Liu, J. Wang, Scalable and biomimetic anti-oil-fouling photothermal fabric for efficient solar-driven interfacial evaporation, *Sep. Purif. Technol.* 312 (2023), 123289.
- [85] W. Wang, J. Niu, J. Guo, L. Yin, H. Huang, In situ synthesis of PPy-Fe_xO_y-CTS nanostructured gel membrane for highly efficient solar steam generation, *Sol. Energy Mater. Sol. Cells* 201 (2019), 110046.
- [86] L. Shi, Y. Shi, S. Zhuo, C. Zhang, Y. Aldrees, S. Aleid, P. Wang, Multi-functional 3D honeycomb ceramic plate for clean water production by heterogeneous photo-Fenton reaction and solar-driven water evaporation, *Nano Energy* 60 (2019) 222–230.
- [87] S. Yan, H. Song, Y. Li, J. Yang, X. Jia, S. Wang, X. Yang, Integrated reduced graphene oxide/polypyrrole hybrid aerogels for simultaneous photocatalytic decontamination and water evaporation, *Appl Catal B: Environ.* 301 (2022), 120820.
- [88] Y. Chen, G. Zhao, L. Ren, H. Yang, X. Xiao, W. Xu, Blackbody-inspired array structural polypyrrole-sunflower disc with extremely high light absorption for efficient photothermal evaporation, *ACS Appl. Mater. Interfaces* 12 (2020) 46653–46660.
- [89] Y. Li, S. Zhang, Z. Xia, L. Wang, J. Fan, Micro-macro-capillaries fabric-based evaporator for eliminating salt accumulation and highly efficient solar steam generation, *Sep. Purif. Technol.* 308 (2023), 122852.
- [90] Y. Xu, J. Ma, Y. Han, H. Xu, Y. Wang, D. Qi, W. Wang, A simple and universal strategy to deposit Ag/polypyrrole on various substrates for enhanced interfacial solar evaporation and antibacterial activity, *Chem. Eng. J.* 384 (2020), 123379.
- [91] Y. Xu, C. Tang, J. Ma, D. Liu, D. Qi, S. You, F. Cui, Y. Wei, W. Wang, Low-tortuosity water microchannels boosting energy utilization for high water flux solar distillation, *Environ. Sci. Tech.* 54 (2020) 5150–5158.
- [92] F. Zhao, X. Zhou, Y. Shi, X. Qian, M. Alexander, X. Zhao, S. Mendez, R. Yang, L. Qu, G. Yu, Highly efficient solar vapour generation via hierarchically nanostructured gels, *Nat. Nanotechnol.* 13 (2018) 489–495.
- [93] R. Li, L. Zhang, L. Shi, P. Wang, MXene Ti₃C₂: An effective 2D light-to-heat conversion material, *ACS Nano* 11 (2017) 3752–3759.
- [94] J. Fang, Q. Liu, W. Zhang, J. Gu, Y. Su, H. Su, C. Guo, D. Zhang, Ag/diatomite for highly efficient solar vapor generation under one-sun irradiation, *J. Mater. Chem. A* 5 (2017) 17817–17821.
- [95] L.Z. Casey Finnerty, D.L. Sedlak, K.L. Nelson, B. Mi, Synthetic graphene oxide leaf for solar desalination with zero liquid discharge, *Environ. Sci. Tech.* 51 (2017) 11701–11709.
- [96] X. Zhou, F. Zhao, Y. Guo, Y. Zhang, G. Yu, A hydrogel-based antifouling solar evaporator for highly efficient water desalination, *Energ. Environ. Sci.* 11 (2018) 1985–1992.
- [97] S. Zhou, S. Huang, Y. Ming, Y. Long, H. Liang, S. Ruan, Y.J. Zeng, H. Cui, A scalable, eco-friendly, and ultrafast solar steam generator fabricated using evolutionary 3D printing, *J. Mater. Chem. A* 9 (2021) 9909–9917.
- [98] Y. Li, S. Yan, X. Jia, J. Wu, J. Yang, C. Zhao, S. Wang, H. Song, X. Yang, Uncovering the origin of full-spectrum visible-light-responsive polypyrrole supramolecular photocatalysts, *Appl Catal B: Environ.* 287 (2021), 119926.

- [99] D. Zhang, Y. Li, X. Chen, C. Li, L. Dong, Z. Wang, Wide spectra-responsive polypyrrole-Ag₃PO₄/BiPO₄ co-coupled TiO₂ nanotube arrays for intensified photoelectrocatalysis degradation of PFOA, *Sep. Purif. Technol.* 287 (2022), 120521.
- [100] L. Midya, A. Chettri, S. Pal, Development of a novel nanocomposite using polypyrrole grafted chitosan-decorated CDs with improved photocatalytic activity under solar light illumination, *ACS Sustain. Chem. Eng.* 7 (2019) 9416–9421.
- [101] N.M. Dimitrijevic, S. Tepavcevic, Y. Liu, T. Rajh, S.C. Silver, D.M. Tiede, Nanostructured TiO₂/polypyrrole for visible light photocatalysis, *J. Phys. Chem. C* 117 (2013) 15540–15544.
- [102] B. Yan, Y. Wang, X. Jiang, K. Liu, L. Guo, Flexible photocatalytic composite film of ZnO-microrods/polypyrrole, *ACS Appl. Mater. Interfaces* 9 (2017) 29113–29119.
- [103] H. Mittal, M. Khanuja, Hydrothermal in-situ synthesis of MoSe₂-polypyrrole nanocomposite for efficient photocatalytic degradation of dyes under dark and visible light irradiation, *Sep. Purif. Technol.* 254 (2021), 117508.
- [104] W. Zhang, L. Wang, D. Zhang, X. Chen, Y. Guan, L. Dong, M. Bao, Y. Li, Bifunctional remediation of oil spills based on pickering emulsification of polypyrrole-Ag₃PO₄/AgCl@Palygorskite, *Sep. Purif. Technol.* 301 (2022), 121943.
- [105] S. Yan, Y. Li, F. Xie, J. Wu, X. Jia, J. Yang, H. Song, Z. Zhang, Environmentally safe and porous MS@TiO₂@PPy monoliths with superior visible-light photocatalytic properties for rapid oil–water separation and water purification, *ACS Sustain. Chem. Eng.* 8 (2020) 5347–5359.
- [106] A.R. Singh, P.S. Dhumal, M.A. Bhakare, K.D. Lokhande, M.P. Bondarde, S. Some, In-situ synthesis of metal oxide and polymer decorated activated carbon-based photocatalyst for organic pollutants degradation, *Sep. Purif. Technol.* 286 (2022), 120380.
- [107] Y. Zhang, J. Li, J. Bai, L. Li, L. Xia, S. Chen, B. Zhou, Dramatic enhancement of organics degradation and electricity generation via strengthening superoxide radical by using a novel 3D AQS/PPy-GF cathode, *Water Res.* 125 (2017) 259–269.
- [108] A. Ait El Fakir, Z. Anfar, A. Amedlous, M. Zbair, Z. Hafidi, M. El Achouri, A. Jada, N. El Alem, Engineering of new hydrogel beads based conducting polymers: metal-free catalysis for highly organic pollutants degradation, *Appl Catal B: Environ.* 286 (2021), 119948.
- [109] X. Zhang, M. Lin, X. Lin, C. Zhang, H. Wei, H. Zhang, B. Yang, Polypyrrole-enveloped Pd and Fe₃O₄ nanoparticle binary hollow and bowl-like superstructures as recyclable catalysts for industrial wastewater treatment, *ACS Appl. Mater. Interfaces* 6 (2014) 450–458.
- [110] Y. Chen, M. Zhang, T. Chen, G. Zhang, H. Xu, H. Sun, L. Zhang, Facile fabrication of rGO/PPy/nZVI catalytic microreactor for ultrafast removal of p-nitrophenol from water, *Appl Catal B: Environ.* 324 (2023), 122270.
- [111] M. Ali, Q. Husain, N. Alam, M. Ahmad, Nano-peroxidase fabrication on cation exchanger nanocomposite: augmenting catalytic efficiency and stability for the decolorization and detoxification of Methyl Violet 6B dye, *Sep. Purif. Technol.* 203 (2018) 20–28.
- [112] M. Abinaya, R. Rajakumaran, S.M. Chen, R. Karthik, V. Muthuraj, In situ synthesis, characterization, and catalytic performance of polypyrrole polymer-incorporated Ag₂MoO₄ nanocomposite for detection and degradation of environmental pollutants and pharmaceutical drugs, *ACS Appl. Mater. Interfaces* 11 (2019) 38321–38335.
- [113] Y. Cheng, Z. Zhao, K. Wu, T. Zou, C. Wang, Q. Zheng, W. Song, Reversal of the photoinduced majority carriers in polypyrrole by semiconductor-insulator-semiconductor heterostructure and related highly-efficient photoreduction of Cr (VI), *Chem. Eng. J.* 393 (2020), 124720.
- [114] Y. Zhang, D. Zhang, L. Zhou, Y. Zhao, J. Chen, Z. Chen, F. Wang, Polypyrrole/reduced graphene oxide aerogel particle electrodes for high-efficiency electrocatalytic synergistic removal of Cr(VI) and bisphenol A, *Chem. Eng. J.* 336 (2018) 690–700.
- [115] C. Chen, K. Li, C. Li, T. Sun, J. Jia, Combination of Pd-Cu catalysis and electrolytic H₂ evolution for selective nitrate reduction using protonated polypyrrole as a cathode, *Environ. Sci. Tech.* 53 (2019) 13868–13877.
- [116] J. Li, H. Liu, X. Cheng, Q. Chen, Y. Xin, Z. Ma, W. Xu, J. Ma, N. Ren, Preparation and characterization of palladium/polypyrrole/foam nickel electrode for electrocatalytic hydrodechlorination, *Chem. Eng. J.* 225 (2013) 489–498.
- [117] J. Li, H. Liu, X. Cheng, Y. Xin, W. Xu, Z. Ma, J. Ma, N. Ren, Q. Li, Stability of palladium-polypyrrole-foam nickel electrode and its electrocatalytic hydrodechlorination for dichlorophenol isomers, *Ind. Eng. Chem. Res.* 51 (2012) 15557–15563.
- [118] J. Wang, C. Cui, Y. Xin, Q. Zheng, X. Zhang, High-performance electrocatalytic hydrodechlorination of pentachlorophenol by amorphous Ru-loaded polypyrrole/foam nickel electrode, *Electrochim. Acta* 296 (2019) 874–881.
- [119] J. Li, H. Wang, Z. Qi, C. Ma, Z. Zhang, B. Zhao, L. Wang, H. Zhang, Y. Chong, X. Chen, X. Cheng, D.D. Dionysiou, Kinetics and mechanisms of electrocatalytic hydrodechlorination of diclofenac on Pd-Ni/PPy-rGO/Ni electrodes, *Appl Catal B: Environ.* 268 (2020), 118696.
- [120] M.J. García-Fernández, M.M. Pastor-Blas, F. Epron, A. Sepúlveda-Escribano, Proposed mechanisms for the removal of nitrate from water by platinum catalysts supported on polyaniline and polypyrrole, *Appl Catal B: Environ.* 225 (2018) 162–171.
- [121] X. Wei, X. Wan, J. Miao, R. Zhang, J. Zhang, Q.J. Niu, Hydrodechlorination of p-chlorophenol on Pd-coated Fe₃O₄@polypyrrole catalyst with ammonia borane as hydrogen donor, *Catal. Lett.* 149 (2019) 823–830.
- [122] C. Lei, Z. Zhou, W. Chen, J. Xie, B. Huang, Polypyrrole supported Pd/Fe bimetallic nanoparticles with enhanced catalytic activity for simultaneous removal of 4-chlorophenol and Cr(VI), *Sci. Total Environ.* 831 (2022), 154754.
- [123] B. Bideau, J. Bras, S. Saini, C. Daneault, E. Loranger, Mechanical and antibacterial properties of a nanocellulose-polypyrrole multilayer composite, *Mater. Sci. Eng.: C* 69 (2016) 977–984.
- [124] M. Maruthapandi, A.P. Nagvenkar, I. Perelshtein, A. Gedanken, Carbon-dot initiated synthesis of polypyrrole and polypyrrole@CuO micro/nanoparticles with enhanced antibacterial activity, *ACS Appl. Polym. Mater.* 1 (2019) 1181–1186.
- [125] H. Du, M. Parit, K. Liu, M. Zhang, Z. Jiang, T.S. Huang, X. Zhang, C. Si, Multifunctional cellulose nanopaper with superior water-resistant, conductive, and antibacterial properties functionalized with chitosan and polypyrrole, *ACS Appl. Mater. Interfaces* 13 (2021) 32115–32125.
- [126] F.A.G. da Silva Jr, J.C. Queiroz, E.R. Macedo, A.W.C. Fernandes, N.B. Freire, M. M. da Costa, H.P. de Oliveira, Antibacterial behavior of polypyrrole: the influence of morphology and additives incorporation, *Mat Sci Eng: C* 62 (2016) 317–322.
- [127] J. Sun, B. Zhang, B. Yu, B. Ma, C. Hu, M. Ulbricht, J. Qu, Maintaining antibacterial activity against biofouling using a quaternary ammonium membrane coupling with electropulsion, *Environ. Sci. Tech.* 57 (2023) 1520–1528.
- [128] Z. Liao, X. Fang, J. Li, X. Li, W. Zhang, X. Sun, J. Shen, W. Han, S. Zhao, L. Wang, Incorporating organic nanospheres into the polyamide layer to prepare thin film composite membrane with enhanced biocidal activity and chlorine resistance, *Sep. Purif. Technol.* 207 (2018) 222–230.
- [129] S.Y. Pi, Y. Wang, Y.W. Lu, G.L. Liu, D.L. Wang, H.M. Wu, D. Chen, H. Liu, Fabrication of polypyrrole nanowire arrays-modified electrode for point-of-use water disinfection via low-voltage electroporation, *Water Res.* 207 (2021), 117825.
- [130] P. Shi, C. Wang, J. Sun, P. Lin, X. Xu, T. Yang, Thermal conversion of polypyrrole nanotubes to nitrogen-doped carbon nanotubes for efficient water desalination using membrane capacitive deionization, *Sep. Purif. Technol.* 235 (2020), 116196.
- [131] J. Wang, J. Wang, W. Wang, X. Hu, Y. Deng, H. Wang, Y. Wu, The generation of carbon/oxygen double defects in FeP/CoP-N-C enhanced by β particles for photic driving degradation of levofloxacin, *Sep. Purif. Technol.* 303 (2022), 122186.
- [132] P. Hu, H. Su, Z. Chen, C. Yu, Q. Li, B. Zhou, P.J.J. Alvarez, M. Long, Selective degradation of organic pollutants using an efficient metal-free catalyst derived from carbonized polypyrrole via peroxymonosulfate activation, *Environ. Sci. Tech.* 51 (2017) 11288–11296.